

RESEARCH ARTICLE

The TPR- and J-domain-containing proteins DJC31 and DJC62 are involved in abiotic stress responses in *Arabidopsis thaliana*

Sophie Dittmer, Tatjana Kleine and Serena Schwenkert*

ABSTRACT

Molecular chaperones play an important role during the response to different stresses. Since plants are sessile organisms, they need to be able to adapt quickly to different conditions. To do so, plants possess a complex chaperone machinery, composed of HSP70, HSP90, J proteins and other factors. In this study we characterized DJC31 (also known as TPR16) and DJC62 (also known as TPR15) of *Arabidopsis thaliana*, two J proteins that additionally carry clamp-type tetratricopeptide repeat domains. Using cell fractionation and split GFP, we could show that both proteins are attached to the cytosolic side of the endoplasmic reticulum membrane. Moreover, an interaction with cytosolic HSP70.1 and HSP90.2 could be shown using bimolecular fluorescence complementation. Knockout of both *DJC31* and *DJC62* caused severe defects in growth and development, which affected almost all organs. Furthermore, it could be shown that the double mutant is more sensitive to osmotic stress and treatment with abscisic acid, but surprisingly exhibited enhanced tolerance to drought. Taken together, these findings indicate that DJC31 and DJC62 might act as important regulators of chaperone-dependent signaling pathways involved in plant development and stress responses.

KEY WORDS: Chaperone, Endoplasmic reticulum, Tetratricopeptide repeat, J domain, Abiotic stress, *Arabidopsis*

INTRODUCTION

Being sessile organisms, plants are exposed to a number of environmental stresses, such as changes in temperature, drought, salinity or pathogen attack. In order to combat these challenges, plants have assembled a plethora of cellular mechanisms to minimize damage and to enable them to recover from exposure to stressors. One such molecular response is the upregulation of heat shock proteins (HSPs), so called molecular chaperones. These proteins are indispensable to maintain protein homeostasis by regulating many processes, such as protein folding, protein degradation or even transmembrane transport of proteins. In the eukaryotic plant cell, chaperones are found not only in the cytosol, but also in the cellular compartments, such as chloroplasts, mitochondria or the endoplasmic reticulum (ER).

Among the HSP family we find HSP70 proteins (known as DnaK in prokaryotes), HSP90 proteins and the HSP40 proteins, which are


essential co-chaperones. The latter are J-domain-containing proteins that regulate ATP hydrolysis activity as well as substrate release from HSP70 proteins (Kampinga and Craig, 2010). J proteins can be classified into three groups according to their domain composition. Class A and B contain J proteins harboring domains and motifs that are most similar to the *E. coli* DnaJ, the founding member of this protein family. Class C is a more diverse group. Members of this group only have the J domain in common, which can be located N- as well as C-terminally. Besides the J domain, class C J proteins can contain additional domains, like tetratricopeptide repeat (TPR) domains, thioredoxin domains or kinase domains. No general pattern for client recognition by class C J proteins has been determined so far, and they are often specialized to a certain subset of client proteins. Once a client is bound, it is transferred to HSP70, which binds the client upon activation of the ATPase by the J domain (Kampinga and Craig, 2010; Rosenzweig et al., 2019).

While HSP70 proteins appear to interact with all unfolded proteins, HSP90 proteins are thought to act downstream of HSP70 in a more specialized manner. Again, a number of co-chaperones have been identified that assist the function of HSP90 proteins. Many of the HSP90 co-chaperones are TPR-containing proteins. These proteins are involved in a variety of different processes and act as interaction modules or mediators for multiprotein complexes. A TPR domain consists of several TPRs, which each consist of 34 amino acids and share a degenerate consensus sequence (Zeytuni and Zarivach, 2012). The TPR motif adopts a basic helix-turn-helix fold. Due to their antiparallel packing, adjacent TPRs form repeating antiparallel α -helices, which create an overall super-helix structure. This super-helix fold forms concave and convex surfaces, which provide a binding groove for different peptides. The ligands usually do not exhibit similarity in structure or sequence; however, binding of ligands to TPR-containing proteins is usually highly specific (Schopf et al., 2017; Zeytuni and Zarivach, 2012). In cytosolic HSP90 proteins, the C-terminal domain contains a Met-Glu-Glu-Val-Asp (MEEVD) motif, which allows binding to TPR domain-containing co-chaperones. Likewise, cytosolic HSP70 proteins contain a Glu-Glu-Val-Asp (EEVD) motif, also allowing the possibility to interact with TPR proteins (D'Andrea and Regan, 2003).

DJC31 (also known as TPR16, AT5G12430) and DJC62 (also known as TPR15, AT2G41520) were first identified in an *in silico* screening for carboxylate clamp-type TPR proteins in *Arabidopsis* by Prasad et al. as two of 24 newly identified carboxylate clamp-type TPR proteins, and are therefore potential co-chaperones of HSP70 and HSP90 (Prasad et al., 2010). Based on the output of different localization prediction software tools, DJC31 and DJC62 have been predicted to be located either in the chloroplast or in the nucleus (Prasad et al., 2010). Based on this prediction, Chiu et al. included DJC31 and DJC62 in their experiments regarding evolution and function of chloroplast HSP70 proteins and their putative co-chaperones (Chiu et al., 2013). In their study, they

Department Biologie I, Botanik, Ludwig-Maximilians-Universität, Großhaderner Strasse, 2-4, 82152 Planegg-Martinsried, Germany.

*Author for correspondence (serena.schwenkert@lmu.de)

 S.D., 0000-0001-6879-6947; T.K., 0000-0001-6455-3470; S.S., 0000-0003-4301-5176

Handling Editor: John Heath
Received 17 June 2021; Accepted 2 September 2021

performed import experiments with isolated chloroplasts to investigate the predicted plastid localization of 19 J proteins. For DJC31 and DJC62, they could not show successful import of the full-length proteins into the chloroplast. However, C-terminally truncated forms appeared to be imported and processed in the chloroplast in an *in vitro* assay (Chiu et al., 2013). In our study, we aimed to analyze the function of DJC31 and DJC62, revealing that the proteins localize to the cytosolic side of the ER *in vivo*. Moreover, we show that both proteins interact with cytosolic HSP70 and HSP90 proteins, are indispensable for proper development of *Arabidopsis* leaves, roots and flowers, and seem to play a role in osmotic stress tolerance.

RESULTS

DJC31 and DJC62 contain two clamp-type TPR domains as well as J domain

DJC31 and DJC62 are two homologous proteins with 49.4% sequence identity at the protein level in *Arabidopsis thaliana* and are conserved from higher plants to green algae. Moreover, a highly similar structure is predicted for DJC31 and DJC62, indicating that the proteins might be redundant in function. Seven and six TPRs are predicted in the C-terminal half of DJC31 and DJC62, respectively. Three TPRs cluster into two regions, thereby forming two typical clamp-type TPR domains in each protein. Interestingly, both proteins also contain a J domain at their extreme C-terminal ends. No known structural features are predicted for the large N-terminus of each protein, instead they show a tendency towards forming intrinsically disordered protein regions (Fig. S1A).

The subcellular localization of DJC31 and DJC62 revisited

Previously, an *in silico* study of *Arabidopsis* TPR proteins has predicted that DJC31 and DJC62 localize either to the nucleus or the chloroplast (Prasad et al., 2010). In a second study, chloroplast import experiments were performed; however, in these experiments only truncated forms of DJC31 and DJC62 could be successfully imported (Chiu et al., 2013). Since the most recent version of TargetP (<http://www.cbs.dtu.dk/services/TargetP/>) does not detect any signal sequences in either of the two proteins, we aimed to validate the localization of DJC31 and DJC62. Firstly, to confirm the potential presence of a chloroplast transit peptide, the first 80 amino acids of DJC31 (DJC31-TP) and DJC62 (DJC62-TP) were fused to GFP and were transiently expressed in tobacco via *Agrobacterium*-mediated transfection. Protoplasts were isolated from transfected leaves and imaged using confocal fluorescence microscopy. However, for both constructs, localization to the chloroplasts could not be observed. DJC31-TP-GFP was visible as spots in the cytosol and the nucleus. DJC62-TP-GFP localized mainly to the nucleus (Fig. S1B). Since the presence of a chloroplast transit peptide could not be confirmed, we performed GFP localization studies with the full-length DJC31 and DJC62 proteins. Unfortunately, fusion constructs of neither DJC31 nor DJC62 with GFP at the C terminus could be detected in tobacco leaves or *Arabidopsis* protoplasts, possibly due to rapid degradation. Therefore, only the N-terminal part was C-terminally fused to GFP. For this, the region before the first TPR domain was chosen, containing 607 and 552 amino acids of DJC31 (DJC31Int) and DJC62 (DJC62Int), respectively. In this case, GFP was mainly observed surrounding the nucleus, with net-like structures extending towards the plasma membrane. Since this pattern indicated localization to the secretory pathway, DJC31Int-GFP and DJC62Int-GFP were co-expressed with compartment markers for the ER and the Golgi in *Arabidopsis* protoplasts by transient

protoplast transfection (Nelson et al., 2007; Saint-Jore-Dupas et al., 2006; Schweiger et al., 2012). For analyzing colocalization with chloroplasts, chlorophyll autofluorescence was used (Fig. 1A; Fig. S1C). Interestingly, an overlay between the GFP signal of DJC31Int-GFP or DJC62Int-GFP and the chlorophyll autofluorescence could not be observed, confirming our earlier result, that DJC31 and DJC62 do not contain a chloroplast transit peptide. Comparing the localization pattern of the ER marker with the GFP signal of DJC31Int-GFP and DJC62Int-GFP showed that both fluorescent signals matched each other, indicating that DJC31 and DJC62 localize to the ER (Fig. 1A). However, comparing the Golgi marker with DJC31Int-GFP and DJC62Int-GFP did not show an overlay of the GFP and mCherry (Golgi marker) signals (Fig. S1C).

To validate this observation for the endogenous proteins on a biochemical level, a western blot was performed with isolated chloroplasts and microsomal membranes using antibodies directed against the N terminus of DJC31 or DJC62 (Fig. 1B). The ER resident HSP70 family protein BiP was used as ER control and the ferredoxin-NADP⁺-oxidoreductase (FNRL1), located in the chloroplast stroma and at the thylakoid membranes, was used as chloroplast control. As it can be seen from the FNR bands, microsomes contained some contamination from plastid membranes, but DJC31 and DJC62 were exclusively detected in microsomal membranes and not in the chloroplast sample (Fig. 1B).

To further strengthen our observations, a microsomal shift assay was performed (Fig. 1C). Since ribosomes are attached to the ER membrane in the presence of Mg²⁺, EDTA treatment detaches ribosomes from the ER and isolated membranes exhibit a shift to lighter density fractions within a linear sucrose gradient (Schweiger et al., 2012). Again, BiP was used as ER luminal control and exhibited a shifted pattern, as expected for ER-resident proteins. Accumulation of BiP in denser fractions was observed in the presence of Mg²⁺, and a shift to lighter density fractions was observed upon treatment with EDTA. A similar behavior was observed for both DJC31 and DJC62, which were detected in higher density fractions if isolated with Mg²⁺ and were shifted to lighter fractions in the presence of EDTA (Fig. 1C). This result clearly confirms a localization of DJC31 and DJC62 to the ER.

DJC31 and DJC62 localize to the cytosolic side of the ER membrane

Usually, proteins located in the ER carry an N-terminal signal peptide, which enables translocation across the membrane and is cleaved off in the ER lumen (Kunze and Berger, 2015). Additionally, many soluble ER resident proteins contain a C-terminal K/HDEL retention motif, which prevents them from being secreted (Robinson and Aniento, 2020). Neither a predictable signal peptide, nor an ER retention motif could be found in the amino acid sequences of DJC31 and DJC62, which raises the question of whether these proteins are located inside the ER lumen or localize to the ER from the cytosolic side. To answer this question, a split-GFP approach was chosen (Xie et al., 2017). The GFP 1–10 fragment was either expressed on its own and thus targeted to the cytosol or was fused to the signal peptide of PATHOGENESIS-RELATED GENE 1 (PR-1, also known as PRB1) at the N terminus and the HDEL ER retention motif at the C terminus (SP-GFP1–10-HDEL). Co-expression with a protein fused to the GFP11 fragment should only show a GFP signal if GFP1–10 or SP-GFP1–10-HDEL and the protein of interest are present in the same compartment. GFP1–10 and SP-GFP1–10-HDEL were co-expressed in tobacco leaves with the

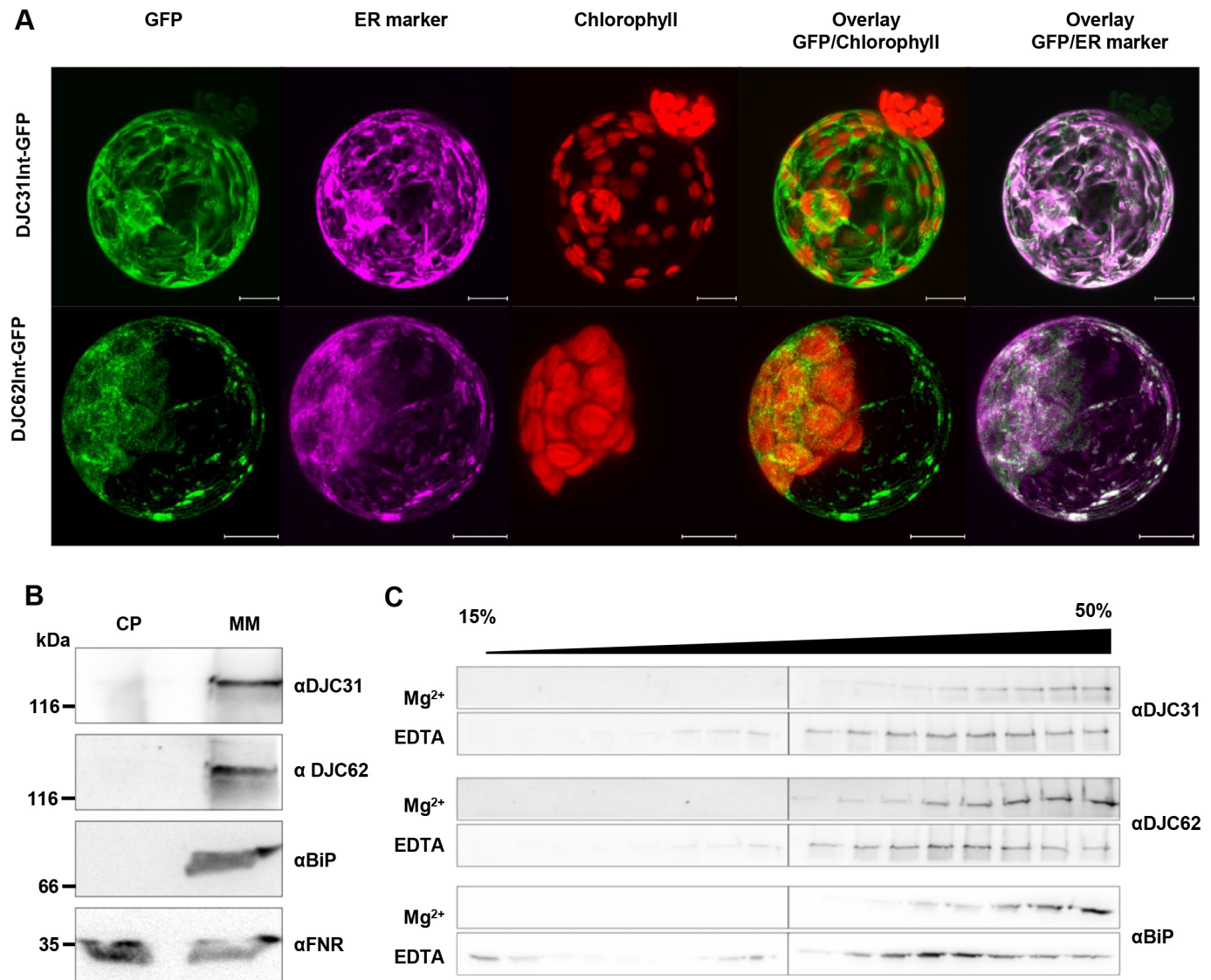


Fig. 1. DJC31 and DJC62 localize to the ER. (A) For determination of the subcellular localization, the N-terminal part of DJC31 and DJC62 (DJC31Int and DJC62Int) were C-terminally fused to GFP (green) and co-expressed with an mCherry-based ER marker (magenta) in *Arabidopsis* protoplasts. Chlorophyll autofluorescence is shown in red. Images are representative of three experiments. Scale bars: 10 μ m. (B) Isolated chloroplasts (CP) and microsomal membranes (MM) were probed with antibodies against DJC31 and DJC62. BiP was used as microsomal control and FNR as chloroplast control. Data are representative of three experiments. (C) Microsomal membranes were isolated with either Mg²⁺ or EDTA. Subsequently, microsomes were loaded onto a linear 15–50% sucrose gradient. Fractions were loaded onto an 8% SDS–PAGE gel and, after western blotting, were probed with specific antibodies against DJC31, DJC62 and BiP as an ER-marker control. The lack of Mg²⁺ in the buffer leads to a shift of the ER membranes to lighter fractions due to removal of ER-associated ribosomes. Data are representative of three experiments.

N-terminal half of either DJC31 or DJC62 carrying GFP11 at the C terminus (DJC31Int–GFP11 or DJC62Int–GFP11, respectively; Fig. 2A). A GFP signal was exclusively observed when DJC31Int–GFP11 or DJC62Int–GFP11 were co-expressed with cytosolic GFP1–10, indicating that DJC31 and DJC62 localize to the cytosolic side of the ER membrane. As positive controls, GFP1–10 and SP–GFP1–10–HDEL were transiently co-expressed in tobacco leaves with GFP11 fusions of either HSP70.1 (also known as HSP70-1), one of the cytosolic HSP70 family proteins, or BiP2, an HSP70 family protein located in the ER lumen. As expected, only co-expression of cytosolic GFP1–10 with GFP11–HSP70.1 and luminal SP–GFP1–10–HDEL with BiP2–GFP11 showed a green fluorescence signal (Fig. 2A).

Predictions of hydrophobicity indicated that DJC31 and DJC62 do not contain transmembrane domains (data not shown). However,

DJC31 and DJC62 could only be detected via western blot in isolated microsomal membranes and not in the soluble fraction. Together with the GFP distribution pattern, these findings nevertheless indicate an attachment of DJC31 and DJC62 to the ER membrane. To analyze this in more detail, isolated microsomes were treated with different agents: Na₂CO₃ for alkaline pH conditions, 1 M NaCl for high salt conditions, 6 M urea for denaturing conditions, 1% SDS to extract integral membrane proteins, and Tris buffer as control. The samples were separated into pellet and soluble fraction via ultracentrifugation and analyzed using immunodetection (Fig. 2B). Isolated microsomes treated with carbonate are known to transform from vesicles into open membrane sheets, releasing proteins that are contained in the vesicle lumen (Fujiki et al., 1982). Furthermore, it has been observed that carbonate can be used to remove ribosomes from

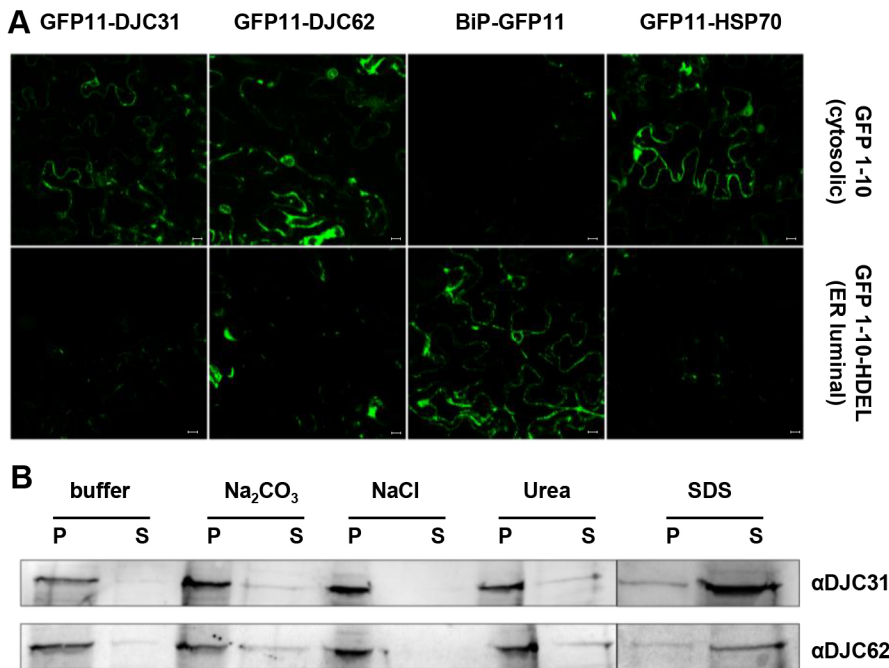


Fig. 2. DJC31 and DJC62 are located on the cytosolic side of the ER membrane. (A) DJC31Int and DJC62Int were C-terminally fused to GFP11 and co-expressed in tobacco leaves either with GFP1-10 (cytosolic) or SP-GFP1-10-HDEL (ER luminal). Cytosolic HSP70.1 and luminal BiP fused to GFP11 were used as controls. Images are representative of three experiments. Scale bars: 10 μ m. (B) Isolated microsomal membranes were incubated in buffer, 0.1 M Na₂CO₃, 1 M NaCl, 6 M urea or 1% SDS for 30 min on ice. After ultracentrifugation, the pellet (P) and soluble (S) fractions were loaded onto an SDS-PAGE gel and, after western blotting, were probed with antibodies against DJC31 and DJC62. Blots are representative of three experiments.

rough ER membranes, indicating that peripherally attached proteins can also be removed using carbonate (Fujiki et al., 1982). Probing carbonate-treated microsomes with antibodies against DJC31 and DJC62 showed that both proteins can partially be removed from the membrane and can be found in the supernatant after ultracentrifugation. A similar result could be obtained under denaturing conditions after treatment with 6 M urea. Applying 1% SDS solubilized the membranes and released most of the DJC31 and DJC62 into the soluble fraction. From this result it can be concluded that DJC31 and DJC62 are peripherally attached to the ER membrane.

The double knockout of *DJC31* and *DJC62* shows growth retardation and a curled leaf phenotype

To analyze the function of DJC31 and DJC62, two knockout lines were isolated carrying T-DNA insertions within the first exon of *DJC31* or the second exon of *DJC62*, respectively. Homozygosity of the T-DNA insertion was confirmed in double- and single-mutant lines by PCR. For verification of T-DNA presence, primers binding within the gene and within the T-DNA insertion were chosen (*DJC31* T-DNA and *DJC62* T-DNA). To confirm homozygosity of the T-DNA, a primer pair spanning the region before and after the T-DNA insertion site was used (*DJC31* gene and *DJC62* gene) (Fig. 3A,B). Knockout of only one gene resulted in a very mild phenotype, which was overall comparable to the wild-type phenotype (Fig. 3C). Therefore, a double mutant was generated by crossing the *djc31* mutant with the *djc62* mutant. The *djc31djc62* double mutant exhibited a strong leaf phenotype, with extremely shortened petioles and shortened, thin, crumpled leaf blades (Fig. 3C). To confirm that these defects were exclusively caused by the knockout of the two genes, the double mutant was complemented with either *DJC31* or *DJC62* under control of a 35S promoter. The *djc31djc62* mutant phenotype was fully rescued by the expression of either gene (Fig. 3C). For the complementation lines, an additional primer pair, with one primer binding within an intron, was designed to discriminate between the endogenous gene and the complementation construct (Fig. 3D). Additionally, all *Arabidopsis* lines were tested at the protein level via

immunodetection using specific DJC31 and DJC62 antisera, to verify absence and presence of the respective gene products (Fig. 3E).

Since *djc31djc62* exhibited drastic morphological changes, we analyzed the phenotype in more detail. The altered leaf morphology of *djc31djc62* was not only visible in rosette leaves but was already present at the cotyledon stage. Although the cotyledons of *djc31djc62* looked similar to wild-type cotyledons in most cases, in 12% of seedlings, heart-shaped cotyledons, bipartite cotyledons or fused cotyledons could be observed (Fig. S2A). Another striking feature of the double mutant was the strong decrease in seed yield, which was scored according to the weight of individual seed batches grown in parallel. The seed yield of *djc31djc62* was decreased by 89%, whereas the seed yields of *djc31* and *djc62* single mutants were decreased by 29% and 25% compared to the wild type, respectively. The reduction in seed yield of the single mutant was not significant compared to the seed yield from wild-type plants, but indicated a trend (Fig. S2B). In addition, the siliques of *djc31djc62* showed an altered morphology. They were much shorter compared to those of wild-type plants, and many siliques had a bent or curled appearance. Siliques of the single mutants were slightly shorter than wild-type siliques, which is consistent with the slightly decreased seed yield (Fig. S2C). Also, flowers of the double mutant showed several different defects. The number of petals, which is typically four for Brassicaceae, was increased or decreased, with petals showing abnormal shapes and fissions. In some flowers, petals were absent completely. Sepals were also affected and showed a difference in size and shape. Furthermore, they did not enclose the flower, as is seen for wild-type flowers, but rather stuck out in different directions. Stamina were shortened or even totally absent. Pistils were bent or had a spiral shape (Fig. S2D). Besides leaves, flowers and siliques, the roots were also affected by the lack of DJC31 and DJC62. Roots of *djc31djc62* plants were extremely shortened and barely showed lateral root growth. The single mutants *djc31* and *djc62* were not significantly reduced in root growth and showed a normal morphology and lateral root formation (Fig. S2E). Since the double mutant exhibited severe growth defects, wild-type and mutant lines were tracked in detail, using a previously published

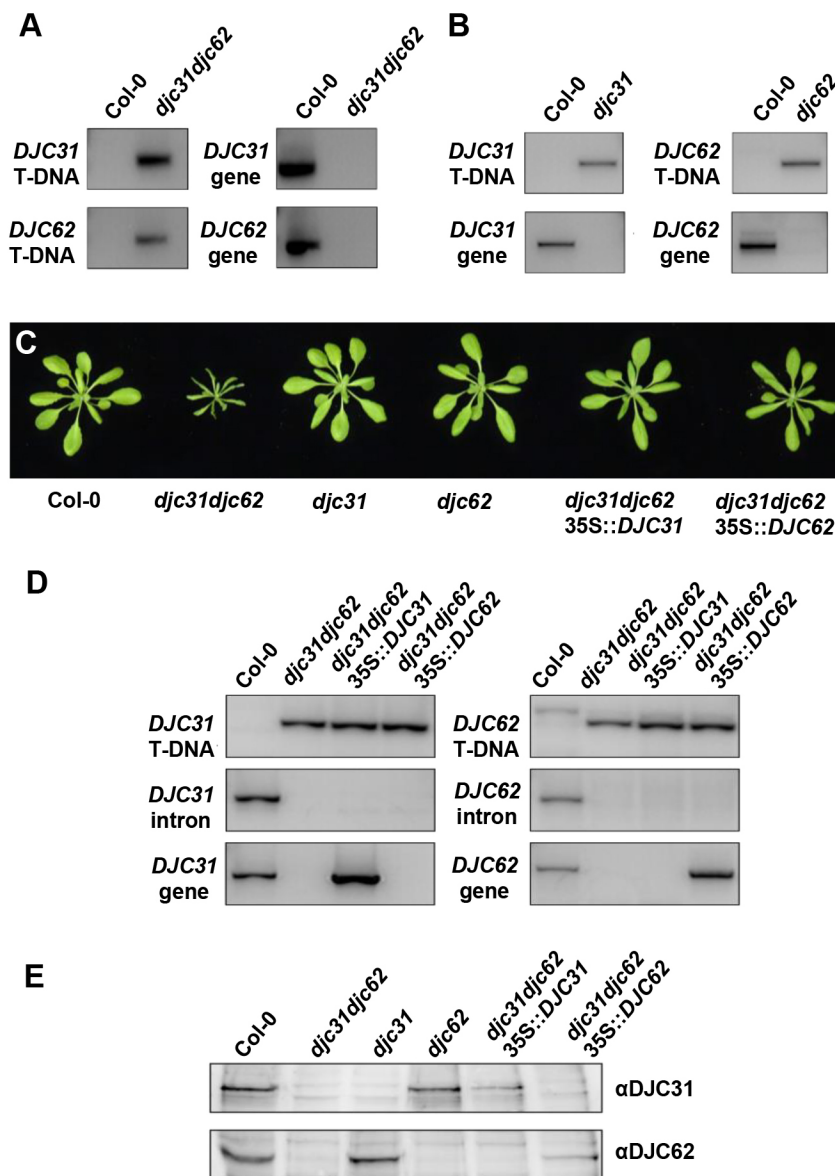


Fig. 3. DJC31 and DJC62 are important for leaf development and growth. (A,B) Wild-type and mutant lines were genotyped to confirm the presence and homozygosity of the T-DNA insertion. (C) Four-week-old wild-type, double-mutant (*djc31djc62*), single-mutant (*djc31* and *djc62*) and complementation (*djc31djc62* 35S::DJC31 and *djc31djc62* 35S::DJC62) lines. The *djc31djc62* mutant has short, thin, crumpled leaves, whereas the single mutants and complementation lines show a phenotype comparable to that of the wild type. The double mutant was obtained by crossing of the single mutants. A representative double homozygous mutant obtained from three individual crosses is shown. A representative line of three individual complementation lines is shown. (D) Wild-type, mutant and complementation lines were genotyped to confirm the presence and homozygosity of the T-DNA insertion and successful genomic integration of the complementation construct. (E) Presence and absence of the respective proteins were analyzed via western blotting, using specific antisera directed against the N termini of DJC31 and DJC62. Data in A,B,D and E are representative of three experiments.

soil-based phenotyping approach (Boyes et al., 2001), whereby growth stages including leaf development, flowering and seed maturation were covered. Plants were discarded when most of the siliques were ready to be harvested. The *djc31djc62* mutant exhibited slower growth in all analyzed growth stages. Strikingly, the total flowering period was tremendously elongated. Rosette leaf growth stages of *djc31* and *djc62* mutants were comparable to those of wild-type plants (Fig. S2F).

DJC31 and DJC62 are potential cytosolic co-chaperones

To investigate whether DJC31 and DJC62 interact with cytosolic chaperones due to the presence of the J domain and the TPR domains, bimolecular fluorescence complementation (BiFC) was performed with cytosolic HSP70.1 and HSP90.2 (also known as HSP90-2). DJC31 and DJC62 were N-terminally fused to the C terminal part of the cyan fluorescent protein SCFP3a (SCFP^C-DJC31 and SCFP^C-DJC62, respectively), and HSP70.1 and HSP90.2 were fused to the N-terminal part of the yellow fluorescent protein Venus (VYNE^N-HSP70.1 and VYNE^N-HSP90.2, respectively). SCFP^C-DJC31 or SCFP^C-DJC62 were

co-transfected in *Arabidopsis* protoplasts with either VYNE^N-HSP70.1 or VYNE^N-HSP90.2, respectively. Interestingly, DJC31 and DJC62 were both observed to interact with HSP70.1 and HSP90.2, suggesting that DJC31 and DJC62 might act as co-chaperones (Fig. 4A). Notably, the interaction was observed in the cytosol, thus strengthening the prior observation that DJC31 and DJC62 face the cytosolic side of the ER membrane.

The main function of the J domain is activating the ATPase domain of HSP70 proteins, thus inducing the chaperone to bind a client protein. Essential for activation of the J domain is the highly conserved HPD motif, which is located between helix II and III (Kampinga and Craig, 2010). Mutating this motif inhibits ATPase activation and generates an inactive co-chaperone. To analyze whether the activation of HSP70 proteins is important for the function of DJC31 and DJC62, loss-of-function mutants were generated by exchanging the histidine of the HPD motif to glutamine (DJC31 H1052Q, DJC62 H1006Q). Subsequently, *djc31djc62* plants were stably transformed with either 35S::DJC31 H1052Q or 35S::DJC62 H1006Q. The loss-of-function variants of DJC31 and DJC62 could not complement the mutant

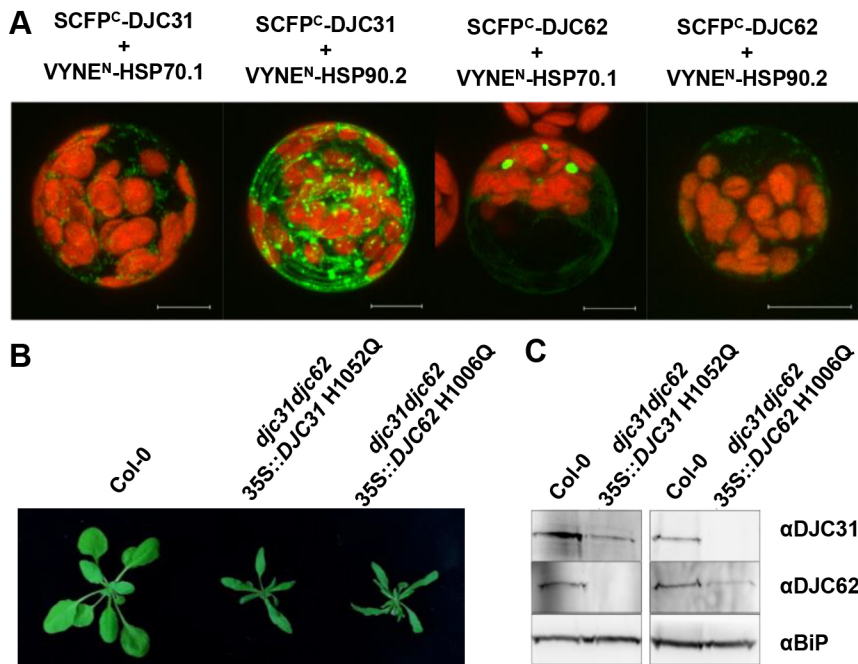


Fig. 4. DJC31 and DJC62 interact with cytosolic HSP70 and HSP90, and interaction with HSP70 is essential for DJC31 and DJC62 function. (A) DJC31 and DJC62 were fused to the C-terminal part of SCFP. HSP70.1 and HSP90.2 were fused to the N-terminal half of VYNE. DJC31 and DJC62 BiFC constructs were co-expressed in *Arabidopsis* protoplasts with either the HSP70.1 or HSP90.2 BiFC construct. Chlorophyll autofluorescence is shown in red. Images are representative of three experiments. Scale bars: 10 μ m. (B) The conserved HPD motif of DJC31 and DJC62 was mutated to QPD to inhibit activation of the HSP70 ATPase domain. Transformation of *djc31djc62* with HPD-mutant constructs could not complement the mutant phenotype. Images show plants at 21 days. A representative line of three individual complementation lines is shown. (C) Presence of the HPD-mutant proteins was confirmed using western blotting. Microsomal membranes isolated from 14-day-old Col-0 and *djc31djc62* 35S::DJC31 H1052Q or *djc31djc62* 35S::DJC62 H1006Q were separated on an SDS-PAGE gel and probed with antibodies against DJC31 and DJC62. BiP was used as loading control. Blots are representative of three experiments.

phenotype of *djc31djc62* (Fig. 4B). To confirm presence of the mutated proteins, a western blot was performed with isolated microsomes, using antibodies against DJC31 and DJC62. BiP was used as loading control (Fig. 4C). This result strongly supports the notion that DJC31 and DJC62 may act as co-chaperones of HSP70 proteins and proves activation of the HSP70 ATPase domain is essential for their function.

Transcriptome changes in *djc31*, *djc62* and *djc31djc62* plants

Since DJC31 and DJC62 might act as co-chaperones and thus be involved in signal transduction and regulation of different transcription factors, transcriptome analysis of wild-type (Col-0), *djc31*, *djc62* and *djc31djc62* plants was performed using RNA sequencing (RNA-Seq). The RNA-Seq analysis revealed substantial changes in gene expression in all mutant plants. Specifically, 1623, 1652 and 1551 genes whose mRNA levels were significantly (at least twofold) changed in *djc31*, *djc62* and *djc31djc62*, respectively, were identified (Fig. 5A; Table S1). Among the reduced transcripts were *DJC31* and *DJC62* themselves, validating the method. To define the overlap of changed transcripts in the different mutants, Venn diagrams were generated, which showed that a significant proportion of genes were regulated in all three mutants with the same overall trend (either reduced or elevated levels; Fig. 5A). Interestingly, the reduction of *HSP70* mRNA levels to 25–30% of wild-type levels seen in the single mutants did not persist in the double mutant (Table S1). Gene Ontology (GO) analysis using DAVID (Huang et al., 2009) showed that indeed genes belonging to the GO terms ‘signal transduction’ and ‘transcription factor’ were enriched in the up- and down-regulated gene lists. Moreover, an enrichment of genes encoding proteins involved in responses to salicylic acid, ethylene and abiotic stresses like salt and cold were identified. Within the ‘cellular component’ GO category, no enrichment could be found for the reduced transcripts of all mutants, but remarkably, the proteins encoded by upregulated transcripts in the *djc62* mutant are found with a 15-fold enrichment in the ER body (Table S2).

To establish a possible link between transcript changes and the *djc31djc62* mutant phenotype, genes that were deregulated exclusively in the double mutant were analyzed separately. Here, the elevated expression of genes encoding proteins participating in hydrogen peroxide metabolism and having peroxidase activity – most of them are extracellular peroxidases – was outstanding (Fig. 5B; Table S2). Additionally, several transcripts encoding proteins involved in root hair tip growth and root development were reduced to 19–30% of wild-type levels; among them *COW1* (*CAN OF WORMS1*, also known as *SFH1*), a phosphatidylinositol transfer protein essential for root hair tip growth (Bohme et al., 2004), and *MYB DOMAIN PROTEIN 77* (*MYB77*), which is involved in lateral root development (Shin et al., 2007). This finding that could explain the root phenotype of the double mutant (Fig. S2E). Notably, also the mRNA levels of several *AGAMOUS-LIKE* genes, among them *AGL3* (also known as *SEPALLATA 4*, *SEP4*) and *AGL24* (Table S1), were reduced. *AGL3* is involved in the development of sepals, petals, stamens and carpels, and *AGL24* is a dosage-dependent mediator of flowering (Ditta et al., 2004; Yu et al., 2002). This in turn correlates with the flower deformation phenotype of the double mutant (Fig. S2D) and the delayed onset of flowering, as well as the elongated flowering period (Fig. S2F).

Moreover, the transcripts that were at least twofold up- or down-regulated, with an adjusted *P*-value of <0.05, in *djc31*, *djc62* and *djc31djc62* samples were analyzed using MapMan (<https://mapman.gabipd.org/de>). All samples showed differences in expression levels, especially for transcription factors and factors involved in protein modification and degradation. The *djc31djc62* mutant exhibited more upregulation in these categories compared to the single mutants. Furthermore, an effect was visible in pathways related to signal transduction. Here, receptor kinases and calcium-mediated signaling processes were particularly affected. Regarding hormonal signaling, the expression levels of genes involved in auxin, ethylene and jasmonate signaling were particularly altered (Fig. S3). Taken together, these transcriptome changes point to a putative role of our investigated DJC proteins in stress responses, possibly by eventually affecting the expression of multiple transcription factors.

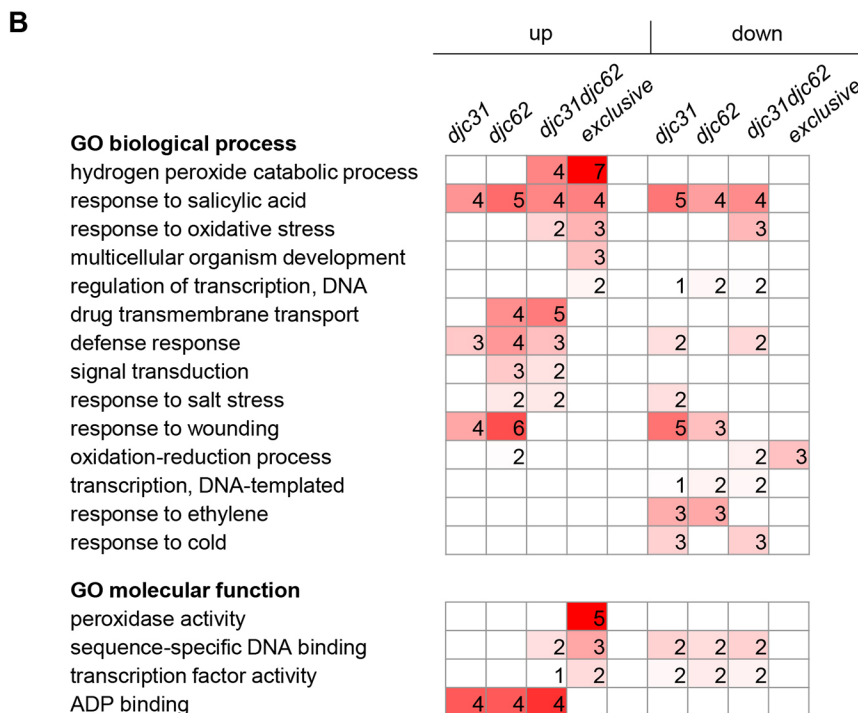
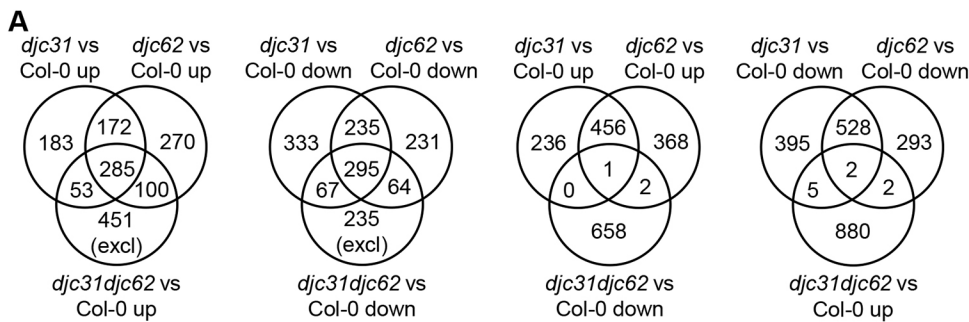


Fig. 5. Changes of transcript accumulation in *djc31*, *djc62* and *djc31djc62* plants. (A) Venn diagrams illustrating shared or unique differentially expressed genes of *djc31*, *djc62* and *djc31djc62* plants, compared to Col-0. Plants were grown on soil until they reached the four-leaves stage. Up and down represents up- and down-regulated mRNA levels compared to Col-0; excl, exclusively regulated in the *djc31djc62* double mutant. (B) Heatmaps illustrating fold enrichment of non-redundant GO term enrichment, which was determined using DAVID (Huang et al., 2009) and REVIGO (Supek et al., 2011). Note, only terms that were enriched in at least one of the gene sets from the *djc31djc62* double mutant but not the single mutants (exclusive) or were enriched in at least two of all the gene sets are shown. The numbers and color code indicate the fold enrichment. White, not enriched.

DJC31 and DJC62 are involved in abiotic stress responses

Due to the observed transcriptional changes in stress response-related transcripts, the effect of different abiotic stress-inducing agents was tested at the phenotypic and molecular level. First, sensitivity to salt stress was analyzed. To examine the effect of NaCl on Col-0, *djc31*, *djc62* and *djc31djc62*, seedlings were grown on MS medium with or without 100 mM NaCl and were phenotypically analyzed after 14 days. Due to the heterogenous growth of the double mutant, the seedlings were analyzed regarding the growth stages they reached. Under non-stressed conditions, almost all Col-0, *djc31* and *djc62* seedlings could reach the four-leaves stage. Growth under salt stress did not affect the germination rate, and the two-leaves stage was reached by almost all seedlings. However, only 45–52% of Col-0, *djc31* and *djc62* seedlings could reach the four-leaves stage within 14 days under salt stress. For the double mutant, a decreased germination rate of 76% was observed under non-stressed conditions as compared to the wild type, as observed previously. Under non-stressed conditions, 45% reached the two-leaves stage and only 28% reached the four-leaves stage. Growth on 100 mM NaCl led to a reduction of the growth rate to 63%, and the two-leaves and four-leaves stages were only reached by 9% and 1%, respectively. This result indicates that DJC31 and DJC62 are involved in processes required to protect the plant against high salinity (Fig. 6A,B).

Besides osmotic stress, the harmful effect of NaCl is also mediated by ionic toxicity. Sodium ions, which are usually present in low concentrations in the cytosol, can compete with potassium ions for binding to different enzymes involved in different cytosolic processes. To exclude that the effect of salt stress was exclusively caused by ionic toxicity, the experiment was repeated using mannitol as inducer of osmotic stress. After 14 days treatment with 3% mannitol, Col-0, *djc31* and *djc62* did not show an effect at the cotyledon stage and the two-leaves stage, but the double mutant showed a strong decrease in germination to 59% of the wild-type germination rate, and only a few seedlings were able to proceed to later growth stages. However, the wild-type and single mutants were also affected by the mannitol treatment at the four-leaves stage. For Col-0, more than half of the seedlings were able to reach the four-leaves stage, but for the two single mutants, only ~25% continued growing after the two-leaves stage (Fig. 6C,D). Nevertheless, this result confirms that DJC31 and DJC62 are of special importance for mechanisms involved in the osmotic stress response.

Since osmotic and drought stresses show some overlapping features, it was likely that DJC31 and DJC62 might also play a role in response to water deprivation. To test this hypothesis, Col-0, *djc31*, *djc62* and *djc31djc62* plants were grown under standard conditions for 14 days. Subsequently, water was withdrawn for 21 days. After 7 days, no signs of dryness could be observed at the

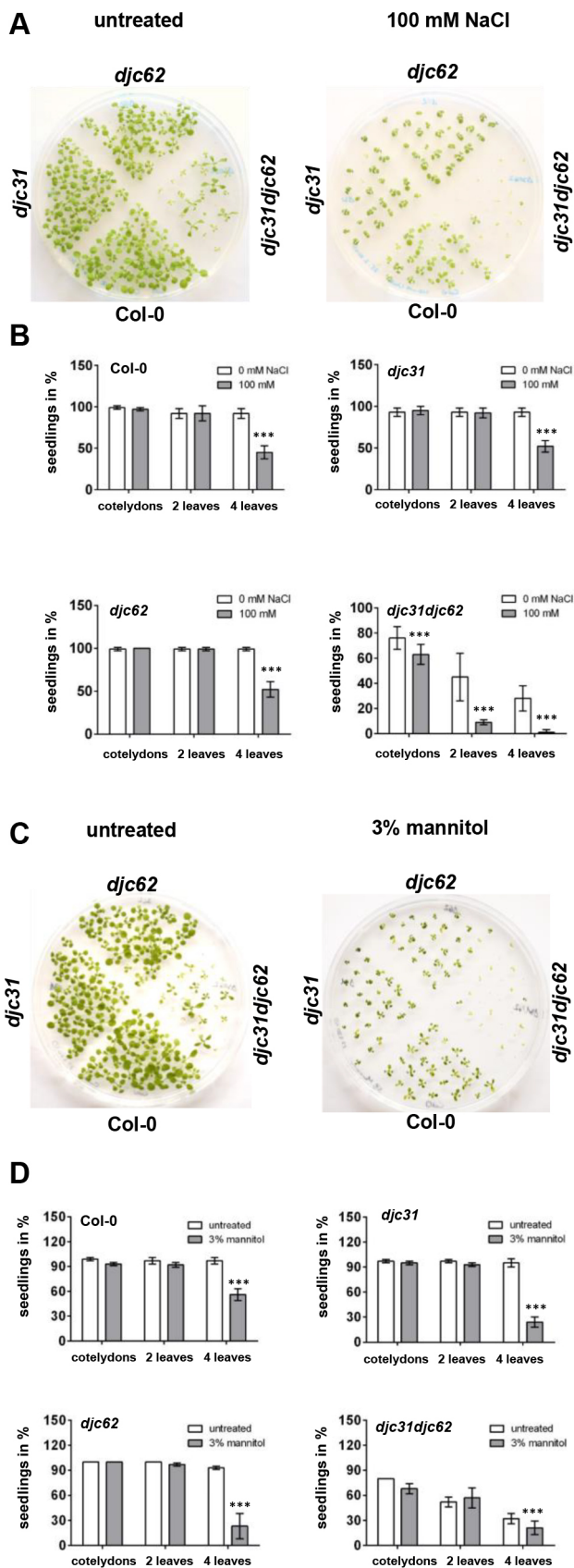


Fig. 6. Growth of wild-type and mutant seedlings under salt and osmotic stress. (A) Col-0, *djc31*, *djc62* and *djc31djc62* were grown on $\frac{1}{2}$ MS medium containing 100 mM NaCl for 14 days. (B) Quantification of growth stages reached by day 14 for the different genotypes under 0 mM NaCl (white) and 100 mM NaCl (gray). Error bars represent the s.d. $n=75$ seedlings per genotype. (C) Col-0, *djc31*, *djc62* and *djc31djc62* were grown on $\frac{1}{2}$ MS medium containing 3% mannitol for 14 days. (D) Quantification of growth stages reached by day 14 for the different genotypes under 0% mannitol (white) or mannitol treatment (gray). Error bars represent the s.d. $n=75$ seedlings per genotype. *** $P<0.001$ (two-tailed, paired *t*-test).

(Fig. 7A). After 21 days, Col-0, *djc31* and *djc62* were completely dry, whereas 75% of the *djc31djc62* plants were still green. Plants were thoroughly watered and examined after 3 days again. The re-watering could not rescue Col-0, *djc31* and *djc62* plants, but surviving *djc31djc62* plants remained viable and started producing flowers (Fig. 7A). Surprisingly, the double mutant turned out to be more drought tolerant than wild-type and single-mutant plants. This result indicates that absence of DJC31 and DJC62 might lead to deregulation of cellular processes, which favors survival under drought conditions, independent of osmotic stress response pathways.

Since we observed that DJC31 and DJC62 localize to the ER membrane but do not contain predicted transmembrane domains, we assumed that the attachment could be transient, and we aimed to analyze whether the proteins could change their subcellular localization under stress conditions such as salt treatment. To this end, DJC31Int-GFP and DJC62Int-GFP, as well as GFP only as control, were transiently co-expressed with an ER marker in tobacco leaves. After protoplast isolation, the protoplasts were incubated with either 150 mM NaCl in W5 buffer, or in W5 buffer without supplements as negative control, for 2 h at room temperature. Intriguingly, under salt stress, DJC31Int-GFP and DJC62Int-GFP seemed to be released from the membrane, forming small spots in the cytosol. The localization pattern of GFP, which could be observed mainly in the cytosol, was comparable between non-stressed and salt-stressed conditions. This result indicates that DJC31 and DJC62 are released from the ER membrane into the cytosol upon induction of salt stress (Fig. 7B).

DJC31 and DJC62 are hypersensitive to ABA

Cellular processes like growth and development, as well as response to stress conditions, are influenced and regulated by different plant hormones. In particular, abscisic acid (ABA) is known to be involved in osmotic and drought stress response. To analyze a potential link between DJC31 and/or DJC62 and ABA signaling, Col-0, *djc31*, *djc62* and *djc31djc62* seedlings were grown on 0.5 μ M ABA. After 14 days, growth was compared between the different genotypes by determination of the growth stages that were reached within this period. Germination was comparable between ABA-treated and untreated seedlings for all genotypes. Non-treated seedlings of Col-0, *djc31* and *djc62* developed as normal. As observed in previous experiments, seedlings of *djc31djc62* showed retarded growth under non-treated conditions. Interestingly, under ABA treatment, almost all seedlings of Col-0 and *djc31* reached the two-leaves stage, whereas for *djc62* a slight reduction was visible. For *djc31djc62*, the number of seedlings reaching the two-leaves stage was tremendously decreased to 10%, whereas under non-treated conditions 44% of the seedlings could reach the two-leaves stage. At the four-leaves stage, the number of seedlings of wild-type plants and single mutants was decreased to 66–74%. Strikingly, for *djc31djc62*, no seedlings reaching the four-leaves stage could be observed under ABA treatment. From this result it can be

leaves. Growth was comparable between wild-type plants and the single mutants. The double mutant showed growth and development as observed before under non-stressed conditions

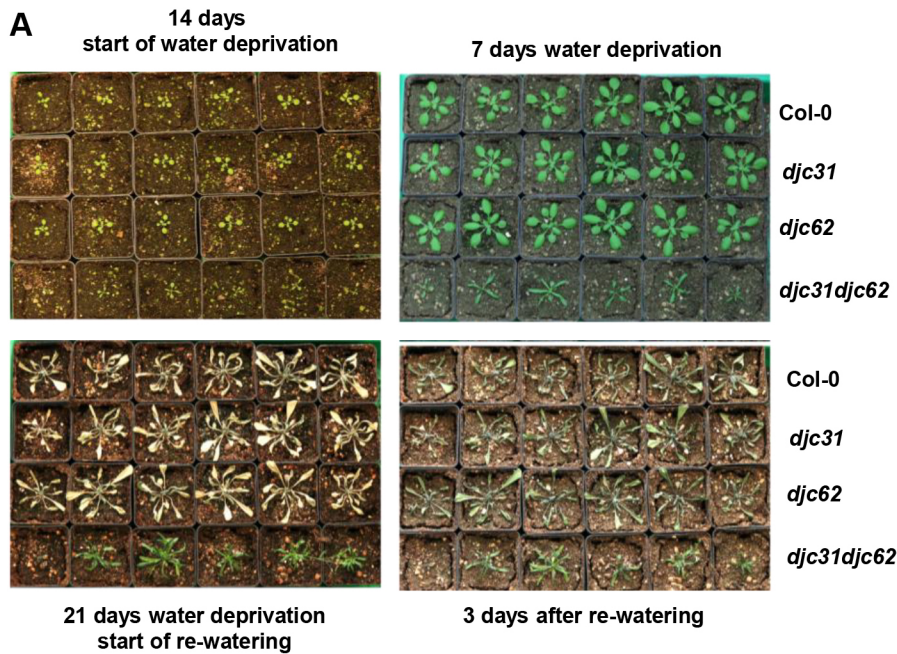
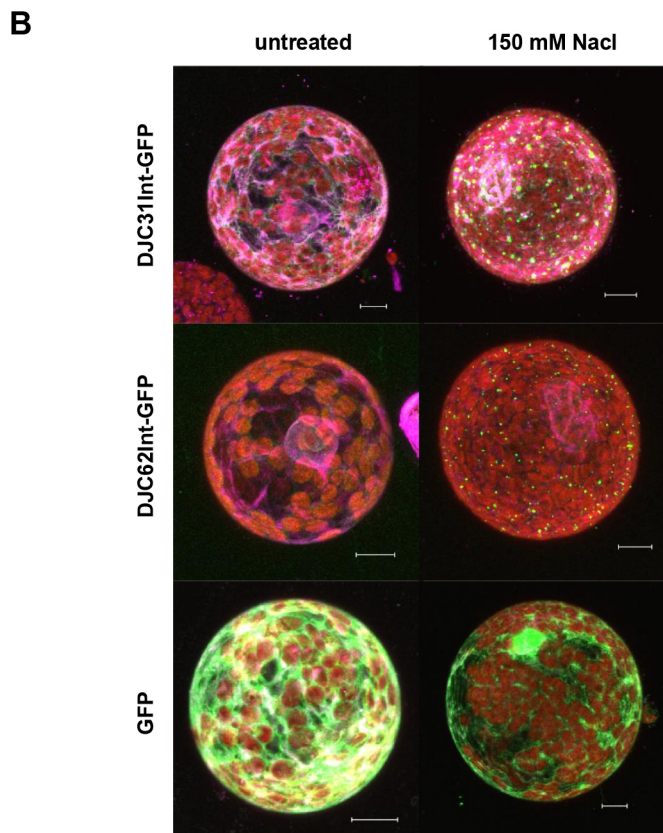


Fig. 7. The *djc31djc62* double mutant is more drought tolerant than wild-type plants, and DJC31 and DJC62 change their subcellular localization under salt stress. (A) Plants were grown on soil for 14 days, after which watering was stopped. After seven days of water deprivation, no signs of dryness or strong growth retardation could be observed. On day 21 of water deprivation, Col-0, *djc31* and *djc62* lines showed a high degree of dryness, whereas the *djc31djc62* plants were still green. After 21 days, the plants were watered again. After 3 days of re-watering Col-0, *djc31* and *djc62* were not able to recover from the water withdrawal, in contrast to *djc31djc62*, for which 75% of the plants survived and remained viable. Images are representative of three experiments. (B) DJC31Int-GFP, DJC62Int-GFP or GFP (green) were co-expressed with an ER marker (magenta) in tobacco. After protoplast isolation, the protoplasts were either incubated with 150 mM NaCl in buffer or only buffer as negative control for 2 h at room temperature. Protoplasts expressing DJC31Int-GFP or DJC62Int-GFP showed formation of fluorescent spots in the cytosol upon salt stress, whereas for GFP the distribution remained comparable between stressed and non-stressed conditions. Chlorophyll autofluorescence is shown in red. Images are representative of three experiments. Scale bars: 10 μ m.



concluded that *djc31djc62* seedlings are hypersensitive to ABA (Fig. 8A,B).

To elucidate whether the observed sensitivity to salt stress is connected to ABA signaling, the expression of *ABA INSENSITIVE 5 (ABI5)* was analyzed. ABI5 is a bZIP transcription factor involved in regulation of ABA signaling (Finkelstein and Lynch, 2000; Park and Kim, 2014). ABI5 expression is activated by drought and salt stress during seed germination, and its activity causes the inhibition

of seed germination or early seedling growth (Skubacz et al., 2016). The expression of *ABI5* was analyzed using qPCR for plants with and without salt treatment. As expected, under salt stress, expression of *ABI5* was twofold induced in Col-0, and interestingly more than threefold induced in *djc31djc62*. Under non-stressed conditions, *ABI5* expression levels were comparable between wild-type plants and the double mutant (Fig. 8C). We therefore conclude that DJC31 and DJC62 play a role in ABA-mediated stress signaling.

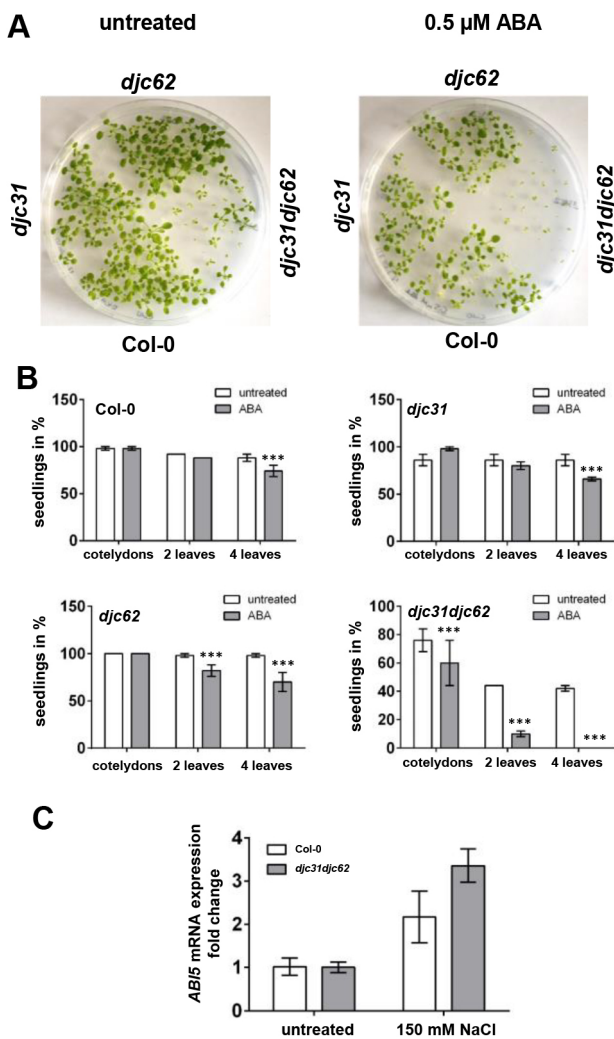


Fig. 8. *djc31djc62* seedlings are sensitive to ABA. (A) Col-0, *djc31*, *djc62* and *djc31djc62* seedlings were grown on ½ MS plates containing 0.5 μM ABA or ethanol as negative vehicle control (untreated) for 14 days. (B) Quantification of growth stages reached by day 14 for the different genotypes under control conditions (white) or ABA treatment (gray). Error bars represent the s.d. $n=50$ seedlings per genotype. *** $P<0.001$ (two-tailed, paired t -test). (C) *djc31djc62* seedlings exhibit enhanced ABA signaling under salt stress. Eight-day-old Col-0 seedlings were treated with 150 mM NaCl for 6 h. After RNA isolation and cDNA synthesis, qPCR analysis was performed. *ABI5* expression was upregulated during salt stress in *djc31djc62* seedlings. Expression of *ABI5* was comparable between Col-0 and *djc31djc62* under non-stressed conditions in eight-day-old seedlings. Mean±s.d. $n=3$. Similar results were obtained in three biological replicates.

DISCUSSION

Chaperones have been described to be involved in a multitude of different processes, such as folding and refolding of proteins, assembly of protein complexes, and protein trafficking and degradation. Additionally, they play a role in response to stress (Rosenzweig et al., 2019). With 18 HSP70 proteins, 118 HSP40 proteins, seven HSP90 proteins, their co-chaperones and other factors, *Arabidopsis thaliana* possesses a complex and versatile chaperone machinery with both overlapping and specialized functions (Craig and Marszalek, 2017; Lin et al., 2001; di Donato and Geisler, 2019). Unfortunately, the interplay of this complex chaperone network as well as precise mechanisms of how chaperones and their co-chaperones are involved in different

cellular processes are barely understood so far. In this work, two HSP40 J proteins, DJC31 and DJC62, were investigated to broaden the understanding of the function and importance of co-chaperones for plant viability.

DJC31 and DJC62 may function as HSP70 and HSP90 co-chaperones at the cytosolic side of the ER membrane

DJC31 and DJC62 were first described in an *in silico* study about carboxylate clamp-type TPR proteins in *Arabidopsis*. Using different localization prediction tools, both proteins were predicted to be located in either the nucleus or the chloroplast (Prasad et al., 2010). Based on this study, Chiu et al. included DJC31 and DJC62 in their study about chloroplast J proteins and determined a plastid localization of both proteins based on chloroplast import experiments (Chiu et al., 2013). However, the import efficiency was rather low, and more than one mature form of the respective protein was observed on the gel after import, whereas the highest bands were close in size to the precursor proteins. To confirm this result, they repeated the import experiment, using truncated versions of the two proteins. Both fragments were imported, but again yielded more than one fragment after processing within the chloroplast. It was concluded that DJC31 and DJC62 are both located in the chloroplast but possess only a very short transit peptide or a transit peptide that is not always removed (Chiu et al., 2013).

Since these previous studies did not provide a clear evidence for a plastid localization, localization studies on DJC31 and DJC62 were reinvestigated in this work using several complementary *in vivo* and *in vitro* approaches. GFP localization studies were performed, using the N-terminal half of DJC31 or DJC62, C-terminally fused to GFP. The two GFP-fusion constructs were co-expressed in *Arabidopsis* protoplasts with fluorescent compartment markers for the ER or Golgi. Overlapping localization patterns could only be observed for DJC31Int-GFP or DJC62Int-GFP and the ER marker, indicating that both proteins localize to the ER. An overlap between the GFP signals and the chlorophyll autofluorescence could not be detected, which supports the idea that DJC31 and DJC62 are not located in the chloroplast. This finding was supported by cell fractionation experiments, including a microsomal shift assay, to specifically identify ER proteins (Schweiger et al., 2012). Moreover, we could show that DJC31 and DJC62 are associated with the ER membrane, despite the lack of hydrophobic segments, in a peripheral manner. DJC31 and DJC62 might be anchored by post-translational modification, which can be reversible in case of S-acylation, or by interaction with proteins in the ER membrane (Chamberlain and Shipston, 2015). Since both modes of attachment can be transient, it raises the question of whether DJC31 and DJC62 are always located at the ER or whether they change their localization under certain circumstances. Such a behavior has previously been described for the cytosolic co-chaperones HOP1, HOP2 and HOP3 in *Arabidopsis*. Under heat stress, HOP1, HOP2 and HOP3 localize to cytoplasmic foci, also known as stress granules, as well as the nucleus. After a recovery period, they return to a diffuse cytoplasmic localization pattern (Fernández-Bautista et al., 2018). Since our experiments revealed DJC31 and DJC62 to be of special importance for the response to osmotic stress, protoplasts co-expressing the N terminus of either DJC31 or DJC62, fused to GFP, together with an ER marker, were treated with NaCl. After 2 h, detachment of the DJC31 and DJC62 fusion proteins from the ER membrane could be observed, with GFP spot formation in the cytosol. This indicated that DJC31 and DJC62 may be released from the ER membrane into the cytosol under stress conditions.

DJC31 and DJC62 are composed of several TPRs in their C-terminal half, which form two TPR domains. Alignments of the two TPR domains with the human HSP70 and HSP90 co-chaperone TPR2 (also known as DNAJC7) show that the TPR domains of DJC31, DJC62 and TPR2 share the conserved K5N9-N6-K2R6 motif, which forms a carboxylate clamp that recognizes the EEVD motif in cytosolic HSP70 and HSP90 chaperones (Brychzy et al., 2003; Prasad et al., 2010). Strikingly, and also similar to TPR2, DJC31 and DJC62 carry a J domain at the C terminus, which is required for activation of the HSP70 ATPase domain (Craig and Marszalek, 2017). This domain composition indicated that DJC31 and DJC62 might act as co-chaperones of both cytosolic HSP70 as well as HSP90. Using BiFC, an interaction with HSP70.1 and HSP90.2 could be experimentally verified for both DJC31 and DJC62. The protein folding pathway is known to include a handover of the client protein from HSP70 to HSP90, which is mediated via HOP proteins (Rosenzweig et al., 2019). The human co-chaperone TPR2 has been found to disrupt the HSP90–client interaction, and by inducing ATP hydrolysis with its J domain, the client is returned to HSP70. It has been proposed that this mechanism constitutes an opportunity for polypeptides that fail to fold properly after the first HSP70–HSP90 cycle to re-enter the cycle, thus reducing the risk of aggregation in the cytosol (Brychzy et al., 2003). Although DJC31 and DJC62 possess a long, disordered N-terminal part, which is not present in TPR2, they are the only cytosolic co-chaperones in *Arabidopsis thaliana* combining two carboxylate clamp-type TPR domains with a J domain (Prasad et al., 2010). Therefore, they might be functional homologs of the human co-chaperone TPR2 and could act in a similar way as mediators between HSP70 and HSP90 to prevent unstable proteins from aggregation and help them to re-enter the folding cycle.

Interestingly, expression of constructs carrying a mutation in the HPD motif in the *djc31djc62* background could not rescue the double-mutant phenotype. Experiments using HPD-motif mutants do not always show this effect, since their function in binding and/or holding a client or in preventing aggregation is more prominent than the dependency as co-chaperone on HSP70 (Kampinga and Craig, 2010). This supports the idea that DJC31 and DJC62 are not predominantly involved in preventing aggregation but that their function is strongly dependent on HSP70 client binding. Failure to rescue the mutant phenotype may be due to DJC31 H1052Q and DJC62 H1006Q mutant proteins disturbing the folding pathway by releasing the client from HSP90 or due to preventing HSP70 binding because of the missing ATPase activation. Additionally, there might be client proteins for which activation or regulation is strictly dependent on the retrograde transfer from HSP90 back to HSP70.

DJC31 and DJC62 are involved in stress responses and hormonal signaling

Chaperones in plants have been described to be involved in responses to various stresses, such as cold and heat stress, drought, osmotic stress, light and pathogens (Jacob et al., 2017). Therefore, the response to different stresses was tested. The *djc31djc62* double-mutant seedlings exhibited enhanced sensitivity to salt stress, whereas single mutants and wild-type seedlings were not affected. Besides osmotic stress, NaCl can also be harmful due to ionic toxicity. Therefore, growth on mannitol, as non-ionic osmotic stress agent, was also tested. Again, *djc31djc62* seedlings were severely affected by the treatment. This indicates that DJC31 and DJC62 are of special importance during osmotic stress. Furthermore, *djc31djc62* plants showed enhanced tolerance to drought, which

was surprising, since the responses to osmotic stress and drought share different regulatory signaling pathways (Zhu, 2002). However, it cannot be excluded that the increased drought tolerance is caused by the aberrant leaf morphology in the mutant.

Moreover, hypersensitivity to ABA was observed for *djc31djc62*, indicating a role in ABA signaling. qPCR expression analysis of *ABI5*, which is involved in ABA signaling and osmotic stress responses (Clément et al., 2011; Park and Kim, 2014), showed that after treatment with 150 mM NaCl for 6 h, *ABI5* was induced twofold in Col-0 but more than threefold in *djc31djc62*. This indicates that ABA signaling is enhanced in *djc31djc62* plants under salt stress. Therefore, the poor growth of the *djc31djc62* mutant under osmotic stress could also be caused by the inhibitory effect of increased ABA levels and its associated pathways.

Interestingly, a similar behavior under osmotic and drought stress has been observed in *Arabidopsis* for mutants of *ATJ1*. *ATJ1* is a J protein that has been reported to localize in mitochondria. *atj1*-mutant seedlings are hypersensitive to glucose and salt, but two-week-old plants on soil show increased tolerance to drought. Furthermore, the *atj1* mutant has been shown to be hypersensitive to ABA (Park and Kim, 2014; Wang et al., 2014). Considering the overlapping findings between *djc31djc62* and mutants of *ATJ1* regarding seedling sensitivity to ABA, salt, glucose and mannitol, and the enhanced drought tolerance, it is conceivable that DJC31 and DJC62 might also likewise be regulators of ABA signaling and developmental or stress-related pathways.

MATERIALS AND METHODS

Plant material and growth conditions

Arabidopsis thaliana ecotype Columbia (Col-0) was used as the wild-type strain. The *djc31djc62 Arabidopsis* double mutant was generated by crossing of *djc31* (SALK_034886) and *djc62* (SALK_050913). The following oligonucleotides were used for genotyping: LBb1.3, 5'-ATT-TTGCCGATTTCGGAAC-3'; DJC31 gene for, 5'-GCAGAATTTGAA-TTCTAGCT-3'; DJC31 gene rev, 5'-ATTTAAATGCATAGAAATAGAC-GAC-3'; DJC62 gene for, 5'-CTAACGGTACTGTGTAGAAG-3'; DJC62 gene rev, 5'-CCAGCTCCGTTAACAACAC-3'; DJC31 intron for, 5'-AC-GTCTCGAGATGAGCAAGTTCGGCGAATTG-3'; DJC31 intron rev, 5'-AGTGCTCAGCCTATGCTTCTTGCCTGCATTA-3'; DJC62 intron for, 5'-ACGTCTCGAGATGTCTCTCTGCGCGGTGGAG-3'; DJC62 intron rev, 5'-GCTGCTCAGCCTAGACATCAGGCATCATCGAT-3'. All complementation constructs were generated by cloning the full-length cDNAs with a stop codon into pB7FWG2 (VIB-UGent Center for Plant Systems Biology). Mutations were inserted by site-directed mutagenesis. *Arabidopsis* seeds were sown either on soil or on sterile solid ½ MS medium (Duchefa Biochemie, Haarlem, The Netherlands). All *Arabidopsis* plants were grown under long-day conditions (day: 16 h, 100 μmol photons m⁻² s⁻¹, 21°C; night: 8 h dark, 16°C) in climate chambers or the greenhouse. *Nicotiana benthamiana* was grown under long-day conditions (day: 16 h, 100 μmol photons m⁻² s⁻¹, 21°C; night: 8 h dark, 16°C) in the greenhouse. Stably transformed *Arabidopsis* plants were generated using the floral dip method using the *Agrobacterium tumefaciens* strain GV3101 (Blum et al., 1987). For selection of transformed plants, 0.8% agar containing ½ MS medium was supplemented with either 25 μg/ml hygromycin (Roche) or 50 μg/ml glufosinate-ammonium (BASTA; Merck, Darmstadt, Germany). For chemical stress treatments, ½ MS medium with 0.8% agar was supplemented with the respective stress-inducing agent. To the non-stressed control plates, the respective solvent was added.

Isolation of microsomal membranes, ER shift analysis and washing of microsomal membranes

Isolation of microsomal membranes and the ER shift assay were performed as described previously (Schweiger et al., 2012). To analyze the attachment of DJC31 and DJC62 to the ER membrane, 80 μg of microsomal

membranes was pelleted at 100,000 *g* for 1 h at 4°C. The pellets were resuspended in different buffers [50 mM Tris-HCl, pH 7.5 (control); 0.1 M Na₂CO₃ (~pH 11); 1 M NaCl in 50 mM Tris-HCl, pH 7.5; 6 M urea in 50 mM Tris-HCl, pH 7.5; 1% SDS in 50 mM Tris-HCl, pH 7.5] and incubated on ice for 30 min. The samples were centrifuged at 100,000 *g*, 4°C for 1 h. The pellet and soluble fractions were loaded onto a 10% SDS-PAGE gel.

Small-scale chloroplast isolation

For small-scale isolation of chloroplasts from *Arabidopsis*, leaves were transferred into a Petri dish with 1 ml isolation buffer (50 mM Tris-HCl, pH 8, 330 mM sorbitol, 0.1 mM EDTA, 0.1% BSA and 1 mM PMSF) on ice. Using a razor blade, the leaves were cut into small pieces. The suspension was filtered through one layer of Miracloth (Calbiochem), rinsed with 1 ml isolation buffer and centrifuged at 1000 *g* for 5 min at 4°C. The supernatant was removed, and the pellet was resuspended in an appropriate volume of isolation buffer.

SDS-PAGE and immunoblotting

SDS-PAGE was performed as described previously (Laemmli, 1970). Proteins, separated via SDS-PAGE, were transferred onto PVDF membranes (Immobilon-P; Millipore, Darmstadt, Germany) via either semi-dry blotting (small proteins) or wet blotting (proteins >100 kDa). Antisera against DJC31 and DJC62 were generated against fragments of the DJC31 and DJC62 N terminus by Eurogentec (Seraing, Belgium). Anti-BiP antibody (α BiP) was purchased from Agrisera (AS09 481; Vännäs, Sweden). FNR antibodies were obtained from Bettina Bölter, LMU Munich (Benz et al., 2009). Antibodies were diluted 1:1000.

Agrobacterium-mediated transient expression of fluorescent proteins in tobacco

For transient transfection of *Nicotiana benthamiana*, the *Agrobacterium* strain AGL1 or GV3101, carrying the respective construct of interest, were cultivated. For split-GFP assays, the respective genes were cloned into vectors obtained from Hans Thordal-Christensen (Xie et al., 2017). Transfection of *Nicotiana benthamiana* leaves and protoplast isolation was performed according to Espinoza-Corral et al. (2019). Analysis by confocal microscopy was performed using the following settings: Leica, TCS SP5; objective lens, HCX PL APO CS; magnification, 63 \times ; numerical aperture, 1.3; imaging medium, glycerol.

Isolation and transfection of *Arabidopsis* protoplasts

For localization experiments, genes were cloned as indicated into pK7FWG2 (VIB-UGent Center for Plant Systems Biology). The Golgi marker corresponds to the cytoplasmic tail and transmembrane domain of soybean α -1,2-mannosidase I, and the ER marker consists of the signal peptide of *A. thaliana* wall-associated kinase 2 at the N-terminus of the fluorescent protein and the ER retention signal His-Asp-Glu-Leu at its C-terminus (Nelson et al., 2007). For BiFC, Gateway vectors were used as described by Gehl et al. (2009). For the isolation of *Arabidopsis* protoplasts, leaves were placed in a Petri dish with 10 ml enzyme solution [1% (w/v) cellulase R10 (Serva, Heidelberg, Germany), 0.3% (w/v) macerozyme R10 (Serva, Heidelberg, Germany), 400 mM mannitol, 20 mM KCl, 20 mM MES pH 5.7, 10 mM CaCl₂ and 0.1% (w/v) BSA], cut into small pieces and incubated in darkness at room temperature for 90 min. Protoplasts were released by gently swirling the Petri dish. The protoplasts were filtered through a nylon mesh (0.4 μ m) and pelleted at 100 *g* for 4 min (low brake). The pellet was resuspended in MMg buffer (0.4 M mannitol, 15 mM MgCl₂ and 4 mM MES pH 5.7). Subsequently, the protoplasts were layered onto a step gradient consisting of 9 ml MSC buffer (10 mM MES pH 5.7, 20 mM MgCl₂ and 120 g/l sucrose, adjusted to 550 mOsm) and 2 ml MMg. After centrifugation at 70 *g* for 10 min, intact protoplasts were transferred into a new tube and diluted with 5 ml W5 buffer (2 mM MES pH 5.7, 154 mM NaCl, 125 mM CaCl₂ and 5 mM KCl). After centrifugation at 100 *g* for 4 min, the pellet was resuspended in 500 μ l MMg. Transfection of *Arabidopsis* protoplasts was performed as described previously, with modifications (Yoo et al., 2007). 10 μ g plasmid DNA was mixed with 100 μ l protoplasts in MMg buffer and 110 μ l PEG solution (40% PEG4000,

0.2 M mannitol and 100 mM CaCl₂). The protoplasts were incubated at room temperature for 15 min. The transfection was stopped by addition of 440 μ l W5 buffer. The samples were centrifuged at 100 *g* for 2 min, the supernatant was removed, and the protoplasts resuspended in 1 ml WI buffer (4 mM MES pH 5.7, 0.5 M mannitol and 20 mM KCl). The transfected protoplasts were incubated at room temperature overnight in the dark.

RNA sequencing

Plants grown on soil at the four-leaves stage were ground in liquid nitrogen. Total RNA from plants was isolated using Trizol (Invitrogen, Carlsbad, USA) and purified using Direct-zol™ RNA MiniPrep Plus columns (Zymo Research, Irvine, USA) according to the manufacturer's instructions. RNA integrity and quality were assessed with an Agilent 2100 Bioanalyzer (Agilent, Santa Clara, USA). Messenger RNA enrichment, generation of mRNA-Seq libraries and 150-bp paired-end sequencing on an Illumina HiSeq 2500 system (Illumina, San Diego, USA) were conducted at Novogene Biotech (Beijing, China) using standard Illumina protocols. Three independent biological replicates were used per genotype. RNA-Seq reads were analyzed on the Galaxy platform (Afgan et al., 2016) essentially as described previously (Xu et al., 2019) with one exception: reads were mapped to the *Arabidopsis* TAIR10 genome with the gapped-read mapper RNA STAR (Dobin et al., 2013) using standard settings. Sequencing data are deposited in the NCBI Gene Expression Omnibus and are accessible through the GEO Series accession number GSE182929.

qPCR analysis

For salt stress treatment followed by qPCR, seven-day-old Col-0 and *djc31djc62* seedlings were transferred into liquid ½MS medium. After 24 h, the medium was exchanged to ½ MS medium containing 150 mM NaCl. ½ MS medium without supplements was used as negative control. After incubation for 6 h, RNA was isolated, reverse transcribed and tested via qPCR with *OEP24B* (oligonucleotides: qOEP24_for: 5'-CTTTACTACTAATTGGACTACTAATA-3' and qOEP24_rev: 5'-GGGACTTTGCGATTTCT-3') as reference gene. For isolation of RNA, plant material was either ground in liquid nitrogen or homogenized using an electronic pestle. Isolation of RNA was performed with the RNeasy Plant Mini Kit (QIAGEN) according to the manufacturer's instructions, including the recommended DNA digestion step using DNaseI (Roche, Mannheim, Germany). For synthesis of cDNA for reverse transcription PCR (RT-PCR), 1 μ g RNA was reverse transcribed using the M-MLV reverse transcriptase (Promega, Mannheim, Germany). For qPCR, cDNA was synthesized by reverse transcription of 1 μ g RNA, using the iScript™ cDNA Synthesis Kit (Bio-Rad, Feldkirchen, Germany). For both enzymes, the recommendations of the manufacturer were followed.

Acknowledgements

Hans Thordal-Christensen (University of Copenhagen, Denmark) is kindly acknowledged for providing split-GFP Gateway vectors. We would like to thank Tamara Bergius and Elisabeth Gerick for excellent technical assistance, as well as Jürgen Soll for helpful discussions.

Competing interests

The authors declare no competing or financial interests.

Author contributions

Conceptualization: S.S.; Methodology: S.D., T.K.; Formal analysis: S.D., T.K.; Investigation: S.D., T.K.; Writing - original draft: S.D., T.K., S.S.; Supervision: S.S.; Funding acquisition: T.K., S.S.

Funding

This work was supported by the Deutsche Forschungsgemeinschaft (DFG; grant numbers CRC 1035, project A04 to S.S.; and CRC TR175, project C01 to T.K.).

Data availability

RNA-sequencing data have been deposited in the NCBI Gene Expression Omnibus and are accessible through the GEO Series accession number GSE182929.

Peer review history

The peer review history is available online at <https://journals.biologists.com/jcs/article-lookup/doi/10.1242/jcs.259032>

References

- Afgan, E., Baker, D., van den Beek, M., Blankenberg, D., Bouvier, D., Čech, M., Chilton, J., Clements, D., Coraor, N., Eberhard, C. et al. (2016). The Galaxy platform for accessible, reproducible and collaborative biomedical analyses: 2016 update. *Nucleic Acids Res.* **44**, W3–W10. doi:10.1093/nar/gkw343
- Benz, J. P., Stengel, A., Lintala, M., Lee, Y.-H., Weber, A., Philipp, K., Gügel, I. L., Kaieda, S., Ikegami, T., Mulo, P. et al. (2009). Arabidopsis Tic62 and ferredoxin-NADP(H) oxidoreductase form light-regulated complexes that are integrated into the chloroplast redox poise. *Plant Cell* **21**, 3965–3983. doi:10.1105/tpc.109.069815
- Blum, H., Beier, H. and Gross, H. J. (1987). Improved silver staining of plant proteins, RNA and DNA in polyacrylamide gels. *Electrophoresis* **8**, 93–99. doi:10.1002/elps.1150080203
- Bohme, K., Li, Y., Charlot, F., Grierson, C., Marrocco, K., Okada, K., Laloue, M. and Nogue, F. (2004). The Arabidopsis COW1 gene encodes a phosphatidylinositol transfer protein essential for root hair tip growth. *Plant J.* **40**, 686–698. doi:10.1111/j.1365-313X.2004.02245.x
- Boyes, D. C., Zayed, A. M., Ascenzi, R., McCaskill, A. J., Hoffman, N. E., Davis, K. R. and Görlach, J. (2001). Growth stage-based phenotypic analysis of Arabidopsis: a model for high throughput functional genomics in plants. *Plant Cell* **13**, 1499–1510. doi:10.1105/TPC.010011
- Brychzy, A., Rein, T., Winklhofer, K. F., Hartl, F. U., Young, J. C. and Obermann, W. M. (2003). Cofactor Tpr2 combines two TPR domains and a J domain to regulate the Hsp70/Hsp90 chaperone system. *EMBO J.* **22**, 3613–3623. doi:10.1093/emboj/cdg362
- Chamberlain, L. H. and Shipston, M. J. (2015). The physiology of protein S-acylation. *Physiol. Rev.* **95**, 341–376. doi:10.1152/physrev.00032.2014
- Chiu, C.-C., Chen, L.-J., Su, P.-H. and Li, H.-M. (2013). Evolution of Chloroplast J Proteins. *PLoS ONE* **8**, e70384. doi:10.1371/journal.pone.0070384
- Clément, M., Leonhardt, N., Droillard, M.-J., Reiter, I., Montillet, J.-L., Genty, B., Laurière, C., Nussaume, L. and Noël, L. D. (2011). The cytosolic/nuclear HSC70 and HSP90 molecular chaperones are important for stomatal closure and modulate abscisic acid-dependent physiological responses in Arabidopsis. *Plant Physiol.* **156**, 1481–1492. doi:10.1104/pp.111.174425
- Craig, E. A. and Marszałek, J. (2017). How do J-proteins get Hsp70 to do so many different things? *Trends Biochem. Sci.* **42**, 355–368. doi:10.1016/j.tibs.2017.02.007
- D'Andrea, L. D. and Regan, L. (2003). TPR proteins: the versatile helix. *Trends Biochem. Sci.* **28**, 655–662. doi:10.1016/j.tibs.2003.10.007
- di Donato, M. and Geisler, M. (2019). HSP90 and co-chaperones: a multitaskers' view on plant hormone biology. *FEBS Lett.* **593**, 1415–1430. doi:10.1002/1873-3468.13499
- Ditta, G., Pinyopich, A., Robles, P., Pelaz, S. and Yanofsky, M. F. (2004). The SEP4 gene of Arabidopsis thaliana functions in floral organ and meristem identity. *Curr. Biol.* **14**, 1935–1940. doi:10.1016/j.cub.2004.10.028
- Dobin, A., Davis, C. A., Schlesinger, F., Drenkow, J., Zaleski, C., Jha, S., Batut, P., Chaisson, M. and Gingeras, T. R. (2013). STAR: ultrafast universal RNA-seq aligner. *Bioinformatics* **29**, 15–21. doi:10.1093/bioinformatics/bts635
- Espinoza-Corral, R., Heinz, S., Klingl, A., Jahns, P., Lehmann, M., Meurer, J., Nicksel, J., Soll, J. and Schwenkert, S. (2019). Plastoglobular protein 18 is involved in chloroplast function and thylakoid formation. *J. Exp. Bot.* **70**, 3981–3993. doi:10.1093/jxb/erz177
- Fernández-Bautista, N., Fernández-Calvino, L., Muñoz, A., Toribio, R., Mock, H. P. and Castellano, M. M. (2018). HOP family plays a major role in long-term acquired thermotolerance in Arabidopsis. *Plant Cell Environ.* **41**, 1852–1869. doi:10.1111/pce.13326
- Finkelstein, R. R. and Lynch, T. J. (2000). The Arabidopsis abscisic acid response gene AB15 encodes a basic leucine zipper transcription factor. *Plant Cell* **12**, 599–609. doi:10.1105/tpc.12.4.599
- Fujiki, Y., Hubbard, A. L., Fowler, S. and Lazarow, P. B. (1982). Isolation of intracellular membranes by means of sodium carbonate treatment: application to endoplasmic reticulum. *J. Cell Biol.* **93**, 97–102. doi:10.1083/jcb.93.1.97
- Gehl, C., Waadt, R., Kudla, J., Mendel, R. R. and Hänsch, R. (2009). New GATEWAY vectors for high throughput analyses of protein-protein interactions by bimolecular fluorescence complementation. *Mol. Plant* **2**, 1051–1058. doi:10.1093/mp/ssp040
- Huang, D. W., Sherman, B. T. and Lempicki, R. A. (2009). Systematic and integrative analysis of large gene lists using DAVID bioinformatics resources. *Nat. Protoc.* **4**, 44–57. doi:10.1038/nprot.2008.211
- Jacob, P., Hirt, H. and Bendahmane, A. (2017). The heat-shock protein/chaperone network and multiple stress resistance. *Plant Biotechnol. J.* **15**, 405–414. doi:10.1111/pbi.12659
- Kampinga, H. H. and Craig, E. A. (2010). The HSP70 chaperone machinery: J proteins as drivers of functional specificity. *Nat. Rev. Mol. Cell Biol.* **11**, 579–592. doi:10.1038/nrm2941
- Kunze, M. and Berger, J. (2015). The similarity between N-terminal targeting signals for protein import into different organelles and its evolutionary relevance. *Front. Physiol.* **6**, 259. doi:10.3389/fphys.2015.00259
- Laemmli, U. K. (1970). Cleavage of structural proteins during the assembly of the head of bacteriophage T4. *Nature* **227**, 680–685. doi:10.1038/227680a0
- Lin, B.-L., Wang, J.-S., Liu, H.-C., Chen, R.-W., Meyer, Y., Barakat, A. and Delseny, M. (2001). Genomic analysis of the Hsp70 superfamily in Arabidopsis thaliana. *Cell Stress Chaperones* **6**, 201–208. doi:10.1379/1466-1268(2001)006<0201:GAOTHS>2.0.CO;2
- Nelson, B. K., Cai, X. and Nebenfuhr, A. (2007). A multicolored set of in vivo organelle markers for co-localization studies in Arabidopsis and other plants. *Plant J.* **51**, 1126–1136. doi:10.1111/j.1365-313X.2007.03212.x
- Park, M. Y. and Kim, S. Y. (2014). The Arabidopsis J protein AtJ1 is essential for seedling growth, flowering time control and ABA response. *Plant Cell Physiol.* **55**, 2152–2163. doi:10.1093/pcp/pcu145
- Prasad, B. D., Goel, S. and Krishna, P. (2010). In silico identification of carboxylate clamp type tetratricopeptide repeat proteins in Arabidopsis and rice as putative co-chaperones of Hsp90/Hsp70. *PLoS ONE* **5**, e12761. doi:10.1371/journal.pone.0012761
- Robinson, D. G. and Aniento, F. (2020). A model for ERD2 function in higher plants. *Front. Plant Sci.* **11**, 343. doi:10.3389/fpls.2020.00343
- Rosenzweig, R., Nillegoda, N. B., Mayer, M. P. and Bukau, B. (2019). The Hsp70 chaperone network. *Nat. Rev. Mol. Cell Biol.* **20**, 665–680. doi:10.1038/s41580-019-0133-3
- Saint-Jore-Dupas, C., Nebenfuhr, A., Boulaflous, A., Follet-Gueye, M. L., Plasson, C., Hawes, C., Driouch, A., Faye, L. and Gomord, V. (2006). Plant N-glycan processing enzymes employ different targeting mechanisms for their spatial arrangement along the secretory pathway. *Plant Cell* **18**, 3182–3200. doi:10.1105/tpc.105.036400
- Schopf, F. H., Biebl, M. M. and Buchner, J. (2017). The HSP90 chaperone machinery. *Nat. Rev. Mol. Cell Biol.* **18**, 345–360. doi:10.1038/nrm.2017.20
- Schweiger, R., Müller, N. C., Schmitt, M. J., Soll, J. and Schwenkert, S. (2012). AtTPR7 is a chaperone docking protein of the Sec translocon in Arabidopsis. *J. Cell Sci.* **125**, 5196–5207. doi:10.1242/jcs.111054
- Shin, R., Burch, A. Y., Huppert, K. A., Tiwari, S. B., Murphy, A. S., Guilfoyle, T. J. and Schachtman, D. P. (2007). The Arabidopsis transcription factor MYB77 modulates auxin signal transduction. *Plant Cell* **19**, 2440–2453. doi:10.1105/tpc.107.050963
- Skubacz, A., Daszkowska-Golec, A. and Szarejko, I. (2016). The role and regulation of ABI5 (ABA-Insensitive 5) in plant development, abiotic stress responses and phytohormone crosstalk. *Front. Plant Sci.* **7**, 1884. doi:10.3389/fpls.2016.01884
- Supek, F., Bošnjak, M., Škunca, N. and Šmuc, T. (2011). REVIGO summarizes and visualizes long lists of gene ontology terms. *PLoS ONE* **6**, e21800. doi:10.1371/journal.pone.0021800
- Wang, X., Jia, N., Zhao, C., Fang, Y., Lv, T., Zhou, W., Sun, Y. and Li, B. (2014). Knockout of AtDJB1, a J-domain protein from Arabidopsis thaliana, alters plant responses to osmotic stress and abscisic acid. *Physiol. Plant* **152**, 286–300. doi:10.1111/ppl.12169
- Xie, W., Nielsen, M. E., Pedersen, C. and Thordal-Christensen, H. (2017). A split-GFP gateway cloning system for topology analyses of membrane proteins in plants. *PLoS ONE* **12**, e0170118. doi:10.1371/journal.pone.0170118
- Xu, D., Marino, G., Klingl, A., Enderle, B., Monte, E., Kurth, J., Hiltbrunner, A., Leister, D. and Kleine, T. (2019). Extrachloroplastic PP7L functions in chloroplast development and abiotic stress tolerance. *Plant Physiol.* **180**, 323–341. doi:10.1104/pp.19.00070
- Yoo, S.-D., Cho, Y.-H. and Sheen, J. (2007). Arabidopsis mesophyll protoplasts: a versatile cell system for transient gene expression analysis. *Nat. Protoc.* **2**, 1565–1572. doi:10.1038/nprot.2007.199
- Yu, H., Xu, Y., Tan, E. L. and Kumar, P. P. (2002). AGAMOUS-LIKE 24, a dosage-dependent mediator of the flowering signals. *Proc. Natl. Acad. Sci. USA* **99**, 16336–16341. doi:10.1073/pnas.212624599
- Zeytuni, N. and Zarivach, R. (2012). Structural and functional discussion of the tetra-trico-peptide repeat, a protein interaction module. *Structure* **20**, 397–405. doi:10.1016/j.str.2012.01.006
- Zhu, J.-K. (2002). Salt and drought stress signal transduction in plants. *Annu. Rev. Plant Biol.* **53**, 247–273. doi:10.1146/annurev.arplant.53.091401.143329

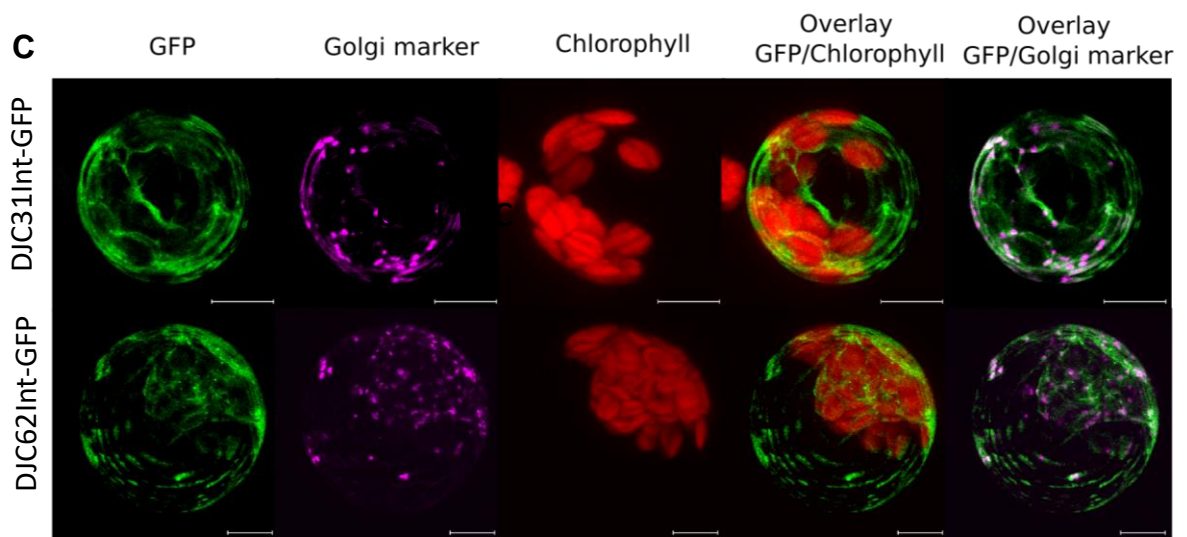
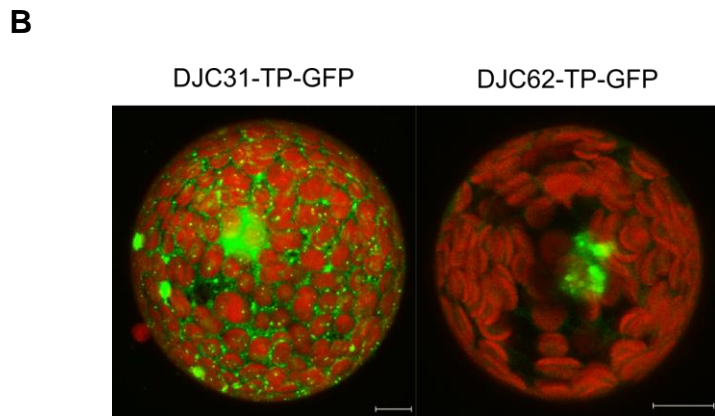
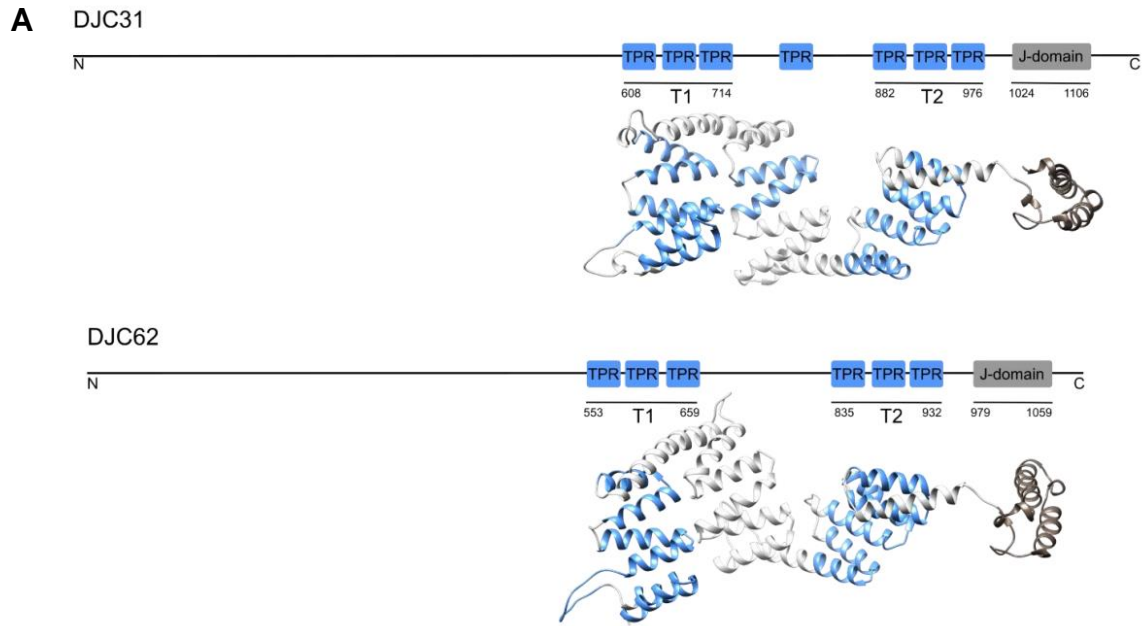


Fig. S1. DJC31 and DJC62 domain structure and expression of DJC31-TP-GFP/DJC62-TP-GFP. **A)** DJC31 and DJC62 are composed of seven and six predicted TPRs (blue), respectively, and a C-terminal J-domain (grey). Both proteins contain a long N-terminal part of unknown structure. Structural models were generated using Phyre2, based on the structure of the human co-chaperone p58IPK. Predicted DJC31 and DJC62 domains are highlighted in blue (TPR repeat) and grey (J-domain). **B)** DJC31 and DJC62 do not contain a chloroplast transit peptide. The first 80 amino acids of DJC31 and DJC62 were C-terminally tagged with GFP and transiently expressed in tobacco. GFP was imaged in protoplasts. DJC31-TP-GFP was observed to be distributed in the cytosol and the nucleus, whereas DJC62-TP-GFP was mainly visible in the nucleus. Scale bar = 10 μ m. **C)** The N-terminal part of DJC31 and DJC62 (DJC31Int and DJC62Int) were C-terminally fused to GFP (green) and co-expressed with an mCherry-based Golgi marker (magenta) in Arabidopsis protoplasts. Chlorophyll autofluorescence is shown in red. Images are representative of three experiments. Scale bars: 10 μ m.

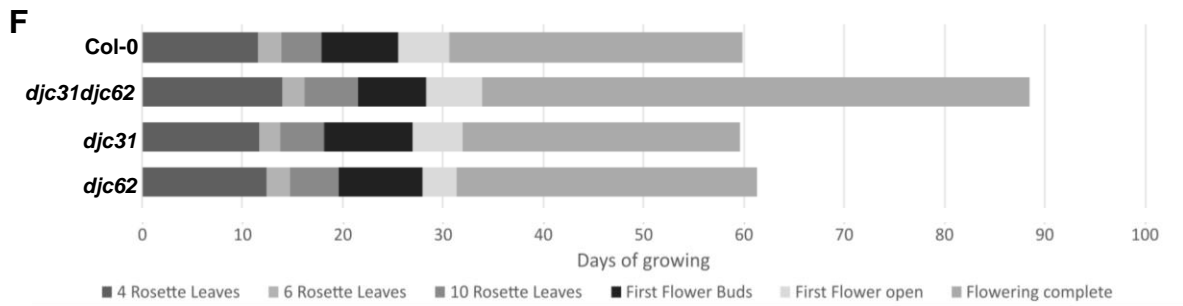
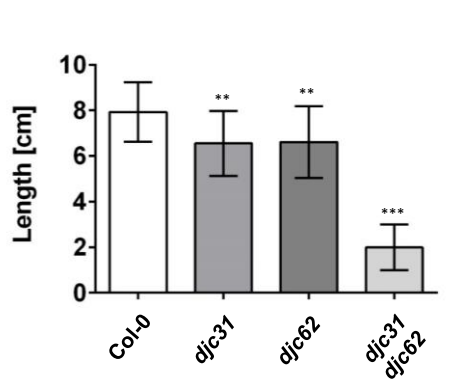
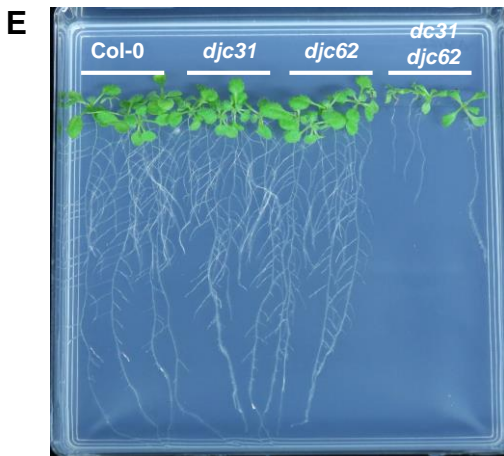
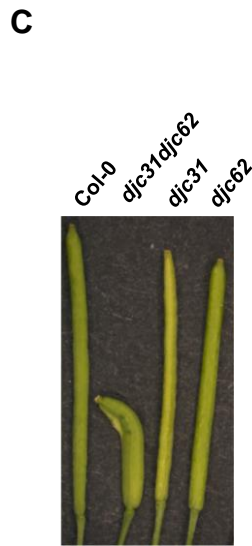
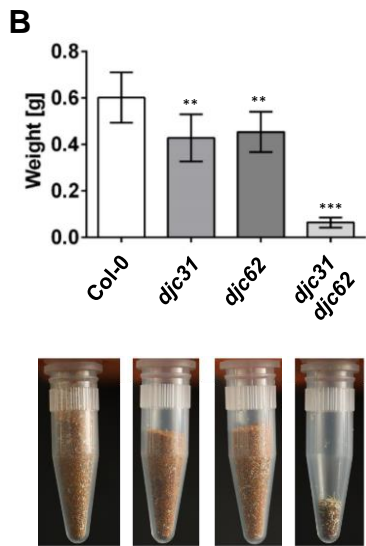


Fig. S2. Phenotype of Col-0, *djc31*, *djc62* and *djc31djc62*. **A)** Photographs of eight days old seedlings of wild type (Col-0), double mutant (*djc31djc62*) and single mutants (*djc31* and *djc62*). The double mutant showed various cotyledon defects. **B)** Seed yield. The amount of seeds in the *djc31djc62* mutant was tremendously decreased, whereas the *djc31* and *djc62* mutants were not significantly decreased in seed yield. Error bars represent the standard deviation, the *t* test was used to indicate significance. Col-0 n=10, *djc31 djc62* n=7, *djc31* n=9, *djc62* n= 10. **C)** Siliques of the *djc31djc62* mutant were shortened and, in some cases, bent or curled. **D)** The *djc31djc62* mutant showed an abnormal flower development. Number and shape of petals were altered or absent. Stamina were shortened or absent. Pistils were bent or curled. Flower morphology of *djc31* and *djc62* was comparable to wild type (Col-0). **E)** The root morphology of *djc31* and *djc62* was comparable to wild type (Col-0), whereas roots of the *djc31djc62* mutant were extremely shortened and barely showed lateral root growth. Error bars represent the standard deviation, the *t* test was used to indicate significance. Col-0 n=18, *djc31 djc62* n= 17, *djc31* and *djc62* n=19. **F)** Soil based phenotyping encompassing leaf development, flower development and silique ripening for wild type (Col-0) double mutant (*djc31djc62*) and single mutants (*djc31* and *djc62*). The growth stages four rosette leaves >1 mm, six rosette leaves >1 mm, ten rosette leaves >1 mm, first flower buds visible, first flower open and flowering complete were chosen, n=25 plants.

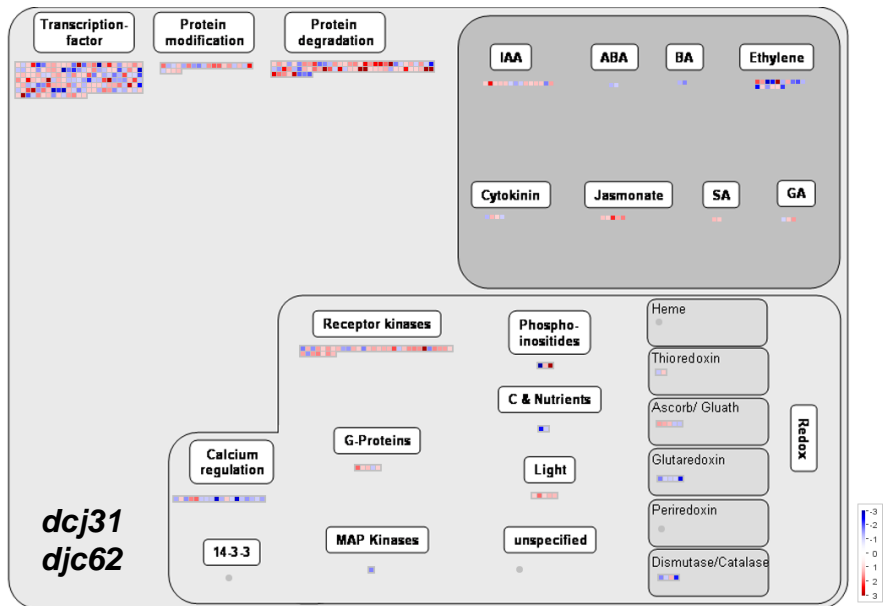
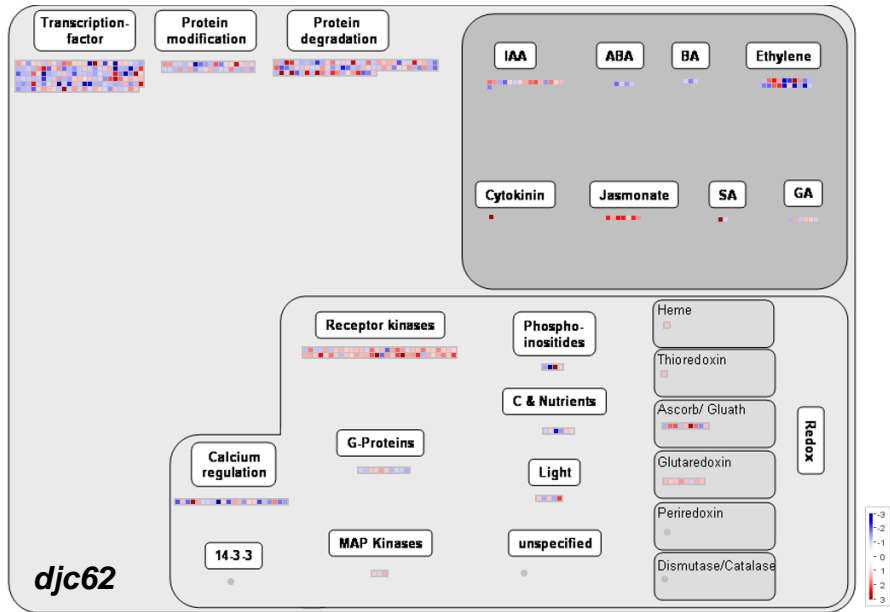
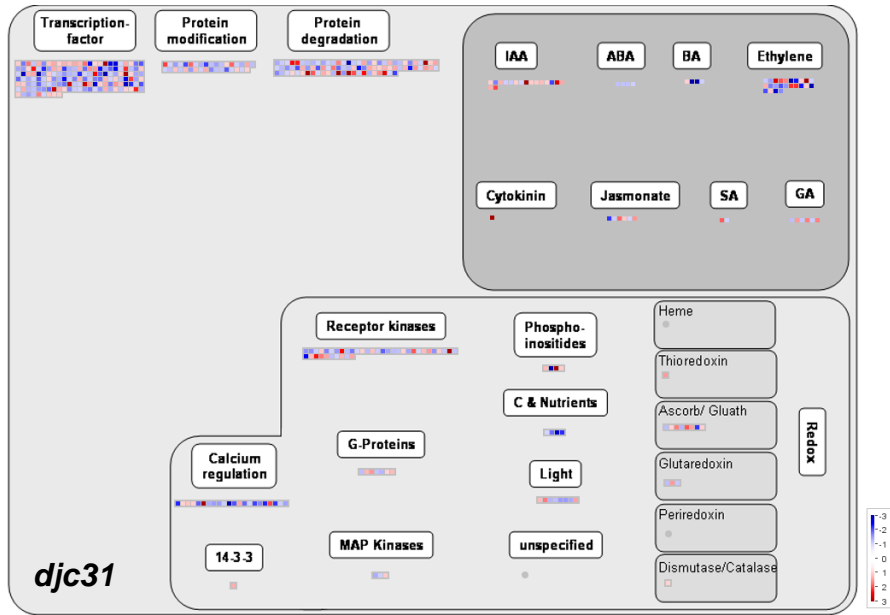


Fig. S3. Overview of regulatory pathways. RNAseq data, showing an at least two-fold up- or downregulation with an adjusted p-value of <0.05 were analyzed regarding their influence on regulatory processes within the cell. The color scale indicates downregulated genes in blue shades and upregulated genes in red shades. Generated with MapMan (<https://mapman.gabipd.org/de>).

Table S1. Genes whose mRNA expression levels changed at least twofold in the *djc31*, *djc62* and *djc31djc62* mutants compared to Col-0.

[Click here to download Table S1](#)

Table S2. GO summary of genes with up- or downregulated mRNA expression levels in the *djc31*, *djc62* and *djc31djc62* mutants compared to Col-0.

[Click here to download Table S2](#)